NASA/CR—1999-209403 NISTIR 6331

Combustion of a Polymer (PMMA) Sphere in Microgravity

Jiann C. Yang, Anthony Hamins, and Michelle K. Donnelly
National Institute of Standards and Technology, Gaithersburg, Maryland

December 1999

The NASA STI Program Office . . . in Profile

Since its founding, NASA has been dedicated to the advancement of aeronautics and space science. The NASA Scientific and Technical Information (STI) Program Office plays a key part in helping NASA maintain this important role.

The NASA STI Program Office is operated by Langley Research Center, the Lead Center for NASA's scientific and technical information. The NASA STI Program Office provides access to the NASA STI Database, the largest collection of aeronautical and space science STI in the world. The Program Office is also NASA's institutional mechanism for disseminating the results of its research and development activities. These results are published by NASA in the NASA STI Report Series, which includes the following report types:

- TECHNICAL PUBLICATION. Reports of completed research or a major significant phase of research that present the results of NASA programs and include extensive data or theoretical analysis. Includes compilations of significant scientific and technical data and information deemed to be of continuing reference value. NASA's counterpart of peer-reviewed formal professional papers but has less stringent limitations on manuscript length and extent of graphic presentations.

- TECHNICAL MEMORANDUM. Scientific and technical findings that are preliminary or of specialized interest, e.g., quick release reports, working papers, and bibliographies that contain minimal annotation. Does not contain extensive analysis.

- CONTRACTOR REPORT. Scientific and technical findings by NASA-sponsored contractors and grantees.

- CONFERENCE PUBLICATION. Collected papers from scientific and technical conferences, symposia, seminars, or other meetings sponsored or cosponsored by NASA.

- SPECIAL PUBLICATION. Scientific, technical, or historical information from NASA programs, projects, and missions, often concerned with subjects having substantial public interest.

- TECHNICAL TRANSLATION. English-language translations of foreign scientific and technical material pertinent to NASA's mission.

Specialized services that complement the STI Program Office's diverse offerings include creating custom thesauri, building customized data bases, organizing and publishing research results . . . even providing videos.

For more information about the NASA STI Program Office, see the following:

- Access the NASA STI Program Home Page at ***http://www.sti.nasa.gov***

- E-mail your question via the Internet to help@sti.nasa.gov

- Fax your question to the NASA Access Help Desk at (301) 621-0134

- Telephone the NASA Access Help Desk at (301) 621-0390

- Write to:
  NASA Access Help Desk
  NASA Center for AeroSpace Information
  7121 Standard Drive
  Hanover, MD 21076

NASA/CR—1999-209403 NISTIR 6331

Combustion of a Polymer (PMMA) Sphere in Microgravity

Jiann C. Yang, Anthony Hamins, and Michelle K. Donnelly
National Institute of Standards and Technology, Gaithersburg, Maryland

Prepared under Interagency Agreement C–32017–C

National Aeronautics and
Space Administration

Glenn Research Center

December 1999

Acknowledgments

This work is supported by NASA Glenn Research Center under NASA Interagency Agreement C-32017-C. The authors would like to thank Mr. Roy McLane for performing some of the parabolic flight experiments, the staff at the NASA-GRC Reduced Gravity Aircraft Facility and the NASA-JSC KC-135 Office for their technical assistance in the parabolic flight experiments, Dr. Howard Ross of GRC, Dr. Liming Zhou of SAIC, Drs. Takashi Kashiwagi and Kathryn Butler of NIST for many stimulating discussions, Ms. Nikki Prive of NIST for analyzing data, and Prof. Seung Baek, a NIST Guest Researcher from the Korea Advanced Institute of Science and Technology for reading parts of the manuscript and for providing many useful comments. This report is dedicated to the memory of Mr. Michael Glover of NIST who fabricated many of the experimental components and who enthusiastically performed several of the parabolic flight experiments.

Available from

NASA Center for Aerospace Information
7121 Standard Drive
Hanover, MD 21076
Price Code: A03

National Technical Information Service
5285 Port Royal Road
Springfield, VA 22100
Price Code: A03

CONTENTS

ABSTRACT

A series of low gravity experiments were conducted to investigate the combustion of supported thermoplastic polymer spheres under varying ambient conditions. The three types of thermoplastic investigated were polymethylmethacrylate (PMMA), polypropylene (PP), and polystyrene (PS). The low gravity environment was achieved by performing the experiments aboard the NASA DC-9 and the KC-135 Reduced Gravity Aircraft. Spheres with diameters ranging from 2 mm to 6.35 mm were tested yielding Grashof numbers calculated to be less than 0.1. The polymer sphere was supported using a 75 μm diameter Al/Cr/Fe alloy wire. The total initial pressure varied from 0.05 MPa to 0.15 MPa whereas the ambient oxygen concentration varied from 19 % to 30 % (by volume). The ignition system consisted of a pair of retractable energized coils. Two CCD cameras recorded the burning histories of the spheres.

The video sequences revealed a number of dynamic events including bubbling and sputtering, as well as soot shell formation and break-up during combustion of the spheres at reduced gravity. The ejection of combusting material from the burning spheres represents a fire hazard that must be considered at reduced gravity. The ejection was found to be sensitive to polymer type, but independent of oxygen concentration and pressure. The average value of the ejection frequency was found to be 3 Hz, 5 Hz, and 5 Hz for PMMA, PS, and PP, respectively. The velocities of the ejected material were estimated by tracking the material in two consecutive video frames. For the PP spheres, V_a = 2.3 (± 1.2) cm/s (with 60 events observed). The ejected material appeared to decelerate at an average rate of ≈ 40 cm/s^2, and traverse an average distance of only 8 mm before burning to completion. The V_a for PS and PMMA was not determined because the ejected material was never observed to exist beyond the visible flame of the parent sphere.

The average burning rates were measured to increase with initial sphere diameter and oxygen concentration, whereas the initial pressure had little effect. The three thermoplastic types exhibited different burning characteristics. For the same initial conditions, the burning rate of PP was slower than PMMA, whereas the burning rate of PS was comparable to PMMA. The transient diameter of the burning thermoplastic exhibited two distinct periods: an initial period (enduring approximately half of the total burn duration) when the diameter remained approximately constant, and a final period when the square of the diameter linearly decreased with time. A simple homogeneous two-phase model was developed to understand the changing diameter of the burning sphere. Its value is based on a competition between diameter reduction due to mass loss from burning and sputtering, and diameter expansion due to the processes of swelling (density decrease with heating) and bubble growth. The model relies on empirical parameters for input, such as the burning rate and the duration of the initial and final burning periods.

INTRODUCTION

Fire safety in space capsules, the Space Shuttles, and future permanent space-stations has long been an important and challenging issue. Polymeric materials that are flammable under certain conditions will pose a potential threat to the safety of the crew and the spacecraft. An example is the overheating of a wire with polymeric insulation due to electrical overload (Friedman, 1996). Therefore, an understanding of the combustion characteristics of such materials (*e.g.*, burning rates, ignitability) under different ambient conditions and in a reduced gravity environment is needed so that appropriate fire suppression strategies can be formulated. In addition to its relevance to spacecraft fire safety, the combustion of polymeric materials is also associated with many applications including solid and hybrid rocket propulsion, waste incineration (Chung and Tsang, 1991; Chung and Lai, 1992; Panagiotou and Levendis, 1994; Panagiotou *et al.*, 1994; Panagiotou and Levendis, 1996), and dust explosion research (Hertzberg *et al.*, 1984; Kobayashi *et al.*, 1995; Okuyama *et al.*, 1996).

Polymer combustion is a highly complicated process where chemical reactions may occur not only in the gas phase, but also in the condensed phase as well as at the solid-gas interface (Kashiwagi, 1994). The combustion processes depend strongly on the coupling between the condensed phase and gas phase phenomena. For some polymers, additional complications arise due to the formation of char layers in the condensed phase. For others, the behavior of the condensed phase involves swelling, bubbling, melting, sputtering, and multi-stage combustion (Essenhigh and Dreier, 1969; Waibel and Essenhigh, 1973; Raghunandan and Mukunda, 1977). Some of these features are similar to phenomena observed in coal particle combustion (Wendt, 1980).

The burning rate is a key parameter in the characterization of polymer combustion. It is directly related to heat release and thereby, fire hazard. The burning rate is often used to rank polymer flammability and to evaluate the inhibition of polymer flammability by additives that act as flame retardants (Aseeva and Zaikov, 1981).

Most of the experimental observations presented in this report have been obtained for polymethylmethacrylate (PMMA), which was chosen because of its well-characterized thermophysical properties. Furthermore, the combustion of PMMA is unique in that it is a non-charring thermoplastic, which simplifies an analysis of the experimental data. In addition to using PMMA spheres, several limited sets of experiments have also been performed using two other thermoplastics, polypropylene (PP) and polystyrene (PS), in order to examine the effects of material properties on burning characteristics at reduced gravity. Polypropylene (PP), and polystyrene (PS) were chosen because they have been used as surrogate materials for waste incineration research (Chung and Tsang, 1991; Chung and Lai, 1992; Panagiotou and Levendis, 1994)

A spherical geometry for the sample was used in this study because it represents the simplest possible combustion configuration in reduced gravity, namely a one-dimensional flame system. In addition, a burning thermoplastic sphere is expected to be analogous to the

combustion of a liquid fuel droplet (Essenhigh and Dreier, 1969; Waibel and Essenhigh, 1973; Raghunandan and Mukunda, 1977; Panagiotou and Levendis, 1994), a well-developed field of study (Williams, 1985). Some differences with liquid fuel droplet combustion can also be expected due to the complex condensed phase processes occurring during combustion. Although several studies on the combustion of single thermoplastic spheres at normal gravity have been cited (Essenhigh and Dreier, 1969; Waibel and Essenhigh, 1973; Raghunandan and Mukunda, 1977; Panagiotou and Levendis, 1994; Panagiotou *et al.*, 1994; Panagiotou and Levendis, 1996), only recently have reduced gravity experiments been reported (our work and Okajima *et al.*, 1996).

The difficulty in conducting polymer sphere combustion experiments in normal gravity is that the spherical geometry of the sample can no longer be maintained once dripping of polymer melt occurs due to the action of gravity. The dripping also distorts the flame shape. In addition, the presence of buoyancy causes the flame to be a tear-drop shape, thereby inducing variations in local heat transfer rates from the flame to the polymer surface, which will have a non-uniform effect on the condensed phase processes such as melting and bubbling. These additional factors will render the characterization of polymer combustion, which in itself is a highly complicated process, more difficult experimentally and almost non-tractable numerically. Therefore, a reduced gravity environment will provide a means for eliminating the additional complications caused by the presence of gravity and for obtaining less ambiguous burning rate data.

The main objective of the present work is to examine experimentally the combustion characteristics of the three aforementioned thermoplastics, to obtain their burning rates in low gravity under different ambient oxygen concentrations (19 % to 30% by volume) and total pressures (0.5 MPa to 1.5 MPa), and *to identify any new phenomena in the gas and condensed phases which might occur during combustion in reduced gravity.* It is anticipated that the simple spherical geometry, in conjunction with reduced gravity conditions will facilitate an assessment of the effect of condensed phase behavior on the polymer burning processes and that the measurements can be used as a means to validate polymer combustion models (*e.g.*, Wichman, 1986; Butler, 1997).

LITERATURE REVIEW

Although the combustion of thermoplastics has been extensively reported in the literature using samples with various geometrical configurations, the following review only focuses on thermoplastics in the form of a sphere burning at normal or reduced gravity.

Normal Gravity Studies

The combustion of a thermoplastic polymer sphere in quiescent air was first studied by Essenhigh and Dreier (1969). Spheres with initial diameters between 1 mm and 2 mm were used. The polymer sphere was attached to the tip of a silica fiber or molded around a thermocouple to measure surface temperature during combustion. The sphere was ignited by a pair of heating coils. Eleven thermoplastics (polyethylene, polypropylene, nylon 6,

PMMA, polystyrene-butadiene, polyvinyl acetate, cellulose acetate, polystyrene, polycarbonate, phenolic resin, and polyamide resin) were examined. General observations revealed that there was an initial internal heating period before ignition during which the particle swelled, that melting of the polymer occurred, that the polymer particle attained different shapes (ellipsoidal, spherical segments, or hemispherical) during the course of burning, that internal bubbling caused sputtering of the polymer surface, that either surface or volumetric (occurring throughout the particle) pyrolysis was possible depending on the nature of the polymer, that the flame was closer to the sphere surface compared to a liquid droplet flame, and that polymer combustion rates appeared to follow the classical d^2-*Law* for liquid droplet combustion. For some char-forming polymers, a two-stage combustion behavior was observed, with the initial stage corresponded to the combustion of volatiles and the second stage corresponded to the burning of the residual char.

In a subsequent studies, Waibel and Essenhigh (1973) examined the effect of ambient oxygen concentration (varied from 10 % to 70 % by volume in nitrogen) on the combustion of polymer (nylon, polystyrene, and PMMA) spheres. The combustion of polymer spheres in an oxygen-rich environment was found to have highly luminous flames with a diminished propensity to sooting. The intensity of internal bubbling appeared to increase with ambient oxygen concentration and the internal boiling duration was somewhat shortened by higher oxygen concentrations. However, it was not clear how the bubbling intensity was quantified.

The combustion of polystyrene spheres (with initial diameters from 2 mm to 5 mm, suspended at the tips of two horizontally opposing quartz fibers) in still air was studied by Raghunandan and Mukunda (1977). The spheres were ignited by a heating coil or a pilot flame. Using a series of identical spheres, mass burning histories were obtained by quenching the flames at different times and weighing the quenched spheres. Temperature histories of the cores of the spheres were also measured by molding the spheres on a thermocouple. Their experimental observations revealed swelling of the spheres, smaller flame diameters when compared to liquid droplets with the same initial diameters, sputtering, higher condensed-phase temperature, gas pockets formed inside the spheres, volumetric pyrolysis, and the burning rate constant to be independent of initial diameter. The burning rate constant of polystyrene was a factor of three lower than that obtained by Essenhigh and Dreier (1969).

The combustion behaviors of PE, PP, PS, and PVC particles (in the range of 47 μm - 300 μm) were studied by Panagiotou and co-workers (1994; 1996) under high heating rates and elevated gas temperatures (to simulate a municipal incinerator environment) using a laminar-flow drop-tube furnace. The particles were observed to have burning times comparable to those of light oil droplets. PVC and PS burned with very luminous yellow flames as a result of high soot loadings of these materials. PVC had the highest burning rate and the brightest flame, and PE had the lowest burning rate and the dimmest flame. The burning times were found to increase almost linearly with the initial particle size. The effect of the degree of crosslinking in polystyrene on the combustion behavior was also examined. The total burnout time and the instantaneous flame diameter were found to increase and

decrease, respectively, with increasing crosslinking. Heterogeneous char combustion was only observed in crosslinked particles after extinction of the volatile flames.

Reduced Gravity Studies

Using a drop tower, Okajima *et al.* (1996) studied flame extinction of polypropylene spheres with an initial diameter of 2 mm burning in microgravity with oxygen concentration varying from 17 % (v/v) to 21 % in nitrogen. The combustion of polypropylene followed the classical d^2-*Law* for combustion of liquid fuel droplets. The flame standoff ratio increased initially, then decreased, and did not approach a constant value. Flame extinction was observed only at low oxygen concentration and during the period when the flame standoff ratio was decreasing. However, no ejection of molten particle or vapor from bubble bursting was evident from their photographs.

In addition, it is worthwhile to note that a limited amount of work has been conducted in reduced gravity using PMMA configurations other than a sphere (see *e.g.*, Melikhov *et al.*, 1983; Goldmeer *et al.*, 1993; Olson and Hegde, 1994; Goldmeer *et al.*, 1997).

EXPERIMENTAL APPARATUS

Low Gravity Environment

The reduced gravity environment was achieved by performing experiments aboard the NASA DC-9 Reduced Gravity Aircraft. The time available to carry out the experiments in both the 2.2 s and 5.18 s NASA drop towers is not long enough to observe the burning histories for spheres with initial diameters (> 1.5 mm) used in this study, although the quality of the low G environment in a drop tower (less than 10^{-4} G) is considerably superior to an aircraft flying a parabolic trajectory (10^{-2} G). For all the experiments, the Grashof number (based on initial sphere diameter) was estimated to be less than 0.1.

Suspended Sphere

The polymer spheres were burned in a suspended configuration. Several techniques for fabricating a suspended sphere were attempted. Both K-type thermocouple wire with its junction embedded at the center of the sphere and a special Al/Cr/Fe alloy wire were used to suspend the polymer sphere.

The apparatus for obtaining a suspended sample is shown in Figure 1. A thermocouple or a special alloy wire is stretched horizontally and heated locally (in the case of a thermocouple, near the thermocouple junction) by resistive heating using a 9V battery and a potentiometer to regulate the current through the wire. The sphere which is placed on a three-dimensional translation stage is then slowly positioned toward the heated wire. As the sphere touches the heated wire, part of it softens such that the wire can be easily inserted into the thermoplastic sphere. In the case of a thermocouple, its junction can be positioned at any location inside the sphere. Although local heating of the sphere during the embedding of the thermocouple may alter the properties of the sphere slightly, it is believed that the change is insignificant if the current through the wire can be controlled in such a way that the temperature of the wire is high enough to locally heat the sphere.

Using the above technique, we have successfully embedded 25 μm, 50 μm, and 75 μm thermocouples. Although working with a 12.5 μm thermocouple is possible, it has not been fruitful because of difficulties associated with the fragility of the wire. The technique can also be extended to the suspension of two or more spheres (for studying the interaction between two burning spheres) provided that the wire is strong enough to support the weight of the spheres. In the case of two or more spheres, only one sphere will have the thermocouple junction embedded in it. Thermocouples (75 μm) were only used in the first flight experiments because the temperature measurements obtained cannot be easily interpreted (see Results and Discussion). Alloy wires (75 μm) were used to suspend the polymer spheres in all subsequent parabolic flight experiments. The supported sample is mounted at the center of a removable holder which is placed along two parallel tracks on the combustion chamber wall (see Figure 2).

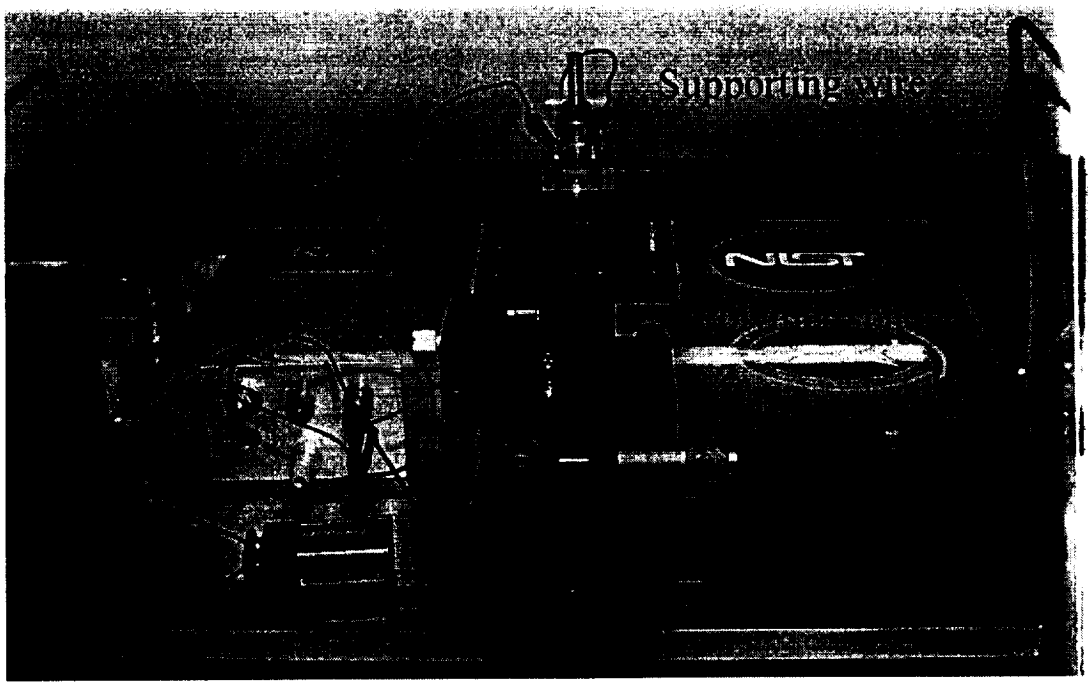

Figure 1. Apparatus for embedding a wire into a thermoplastic sphere.

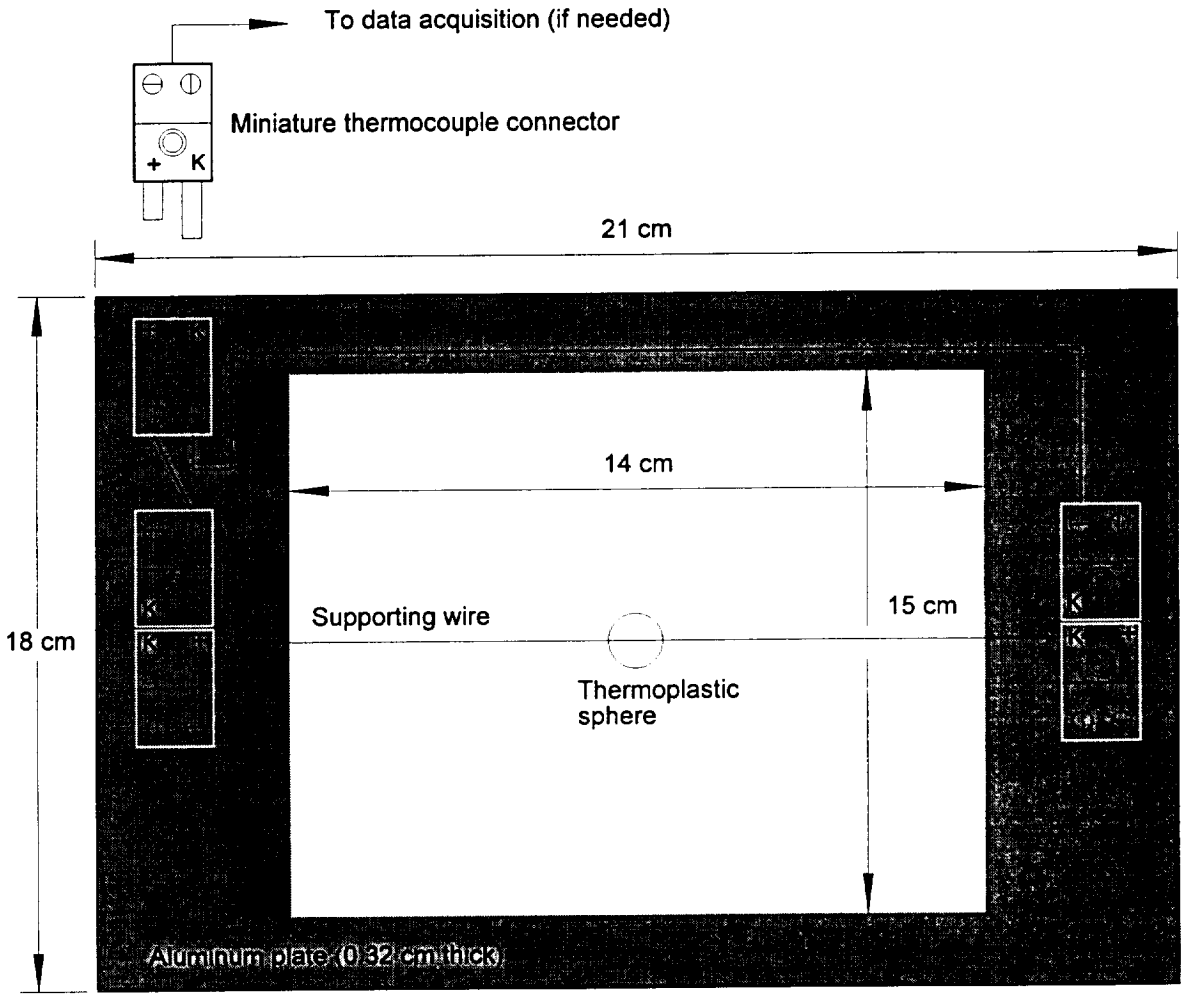

Figure 2. Schematic of a sample holder.

Another technique for embedding a thermocouple has been tried but found to be unreliable. This method involved the dissolution of PMMA powder in toluene (a solvent). An initiator (benzoyl peroxide) was then added to the solution which was then cured in an oven until it became highly viscous. While the solution cured, a thermocouple junction was dipped in and out of the solution periodically and rotated slowly to form a nearly spherical bead. There were still many unresolved technical difficulties. The positioning of the junction in the sphere was not possible, the shape of the PMMA bead was not completely spherical, and bubbles were trapped or formed in the PMMA sphere during the fabrication process. Although two other techniques, gluing of a sphere onto a quartz fiber and injection molding, have been used in previous work (Essenhigh and Dreier, 1969; Waibel and Essenhigh, 1973; Raghunandan and Mukunda, 1977), they have not been considered in this study because the use of injection molding is not practical and attaching a sphere onto a silica fiber requires extreme care in sample handling, a task very difficult to perform during parabolic trajectories.

Ignition System

Although several different ignition methods have been explored (Yang and Hamins, 1995; Yang *et al.*, 1997) in the 1G experiments, two methods for igniting the PMMA spheres have been actively pursued, developed and used in the reduced gravity experiments. These two ignition techniques involve the application of (1) micro-torches and (2) heating coils.

Two opposing micro-torches were used in the first flight experiments in an attempt to ignite the PMMA sphere symmetrically. The micro-torch ignition system consists of a fuel reservoir with a refill port, a stainless steel sub-miniature solenoid valve for initiating the fuel flow, a metering valve, a spark ignition system, and a miniature nozzle. The fuel used is liquefied butane. This fuel was chosen over methane because of its low vapor pressure and ease of refilling. The fuel reservoir is a stainless steel cylinder with an outlet section packed with wicks in order to prevent the fuel from coming out as a flashing liquid. A two-phase fuel flow hinders the smooth operation of the micro-torch. The spark ignition circuit, which is used to ignite the gaseous fuel vapor at the nozzle, is battery operated. The initiation and the duration of the spark discharge can be controlled by the computer *via* a solid state relay. The micro-torch nozzle has a configuration similar to a Bunsen burner. Two identical ignition systems are mounted oppositely on two linear motors which are used for moving the torches toward the sample for ignition and for retracting the torches away from the sample upon ignition.

Although the micro-torch ignition system performed satisfactory, the fuel jet perturbed the flame of the burning PMMA. Consequently, the micro-torches have been replaced by two opposing heating coils. The coils are made of metal alloys with a diameter of 250 μm. The coil was formed by wrapping the wire around a 1 mm diameter screw, yielding a cylindrically shaped coil, approximately 3 mm long and 1.5 mm in diameter. Figure 3 is a schematic of the ignition coil. The coils were mounted on independent, computer controlled motorized linear translation tracks, positioned symmetrically on

opposite sides of the thermoplastic sphere. The coils were oriented with the long axis of the coil perpendicular to the linear track. To ignite a thermoplastic sphere, the coils were resistively heated using a filament transformer. The power to the coils was maintained for a fixed duration (5.5 s) for all experiments, ensuring uniformity of the ignition event. The energized coils were moved toward the sample surface until contact was just made. After contact for 2 s, the coils were slowly (≈ 0.5 cm/s) retracted. Ignition was typically observed 1 s to 2 s after the coil made contact with the sphere, depending on ambient conditions.

The heat flux from the coil was characterized using a small cylindrical Schmidt-Boelter gauge with a flat 6 mm diameter face and a flat spectral response. The coil was positioned to just touch the front of the gauge and the output of the gauge was recorded as the coil was energized. The measurements showed that the flux duration was approximately 6 s, with the average and maximum flux during the 2 s contact period equal to ≈ 340 kW/m^2 and ≈ 380 kW/m^2, respectively.

Flight Package

Figure 4 is a flow diagram indicating individual components of the experimental package. Figure 5 is a photograph of the experimental package (shown inside the aircraft cabin). The experimental hardware was housed inside a rack (60 cm x 60 cm x 106 cm). The hardware consisted of a lap-top computer, a data acquisition and control system used for storing gravity-level information during the experiments and for controlling a pair of micro-step controllers and linear motors (and associated ignition system), a combustion chamber (an interior view is shown in Figure 6), power supplies, two Hi8 mm CCD cameras, two ignition systems, and a vacuum pump. Oxygen/nitrogen mixture cylinders were mounted separately in a gas bottle rack. The combustion chamber was cylindrical, 50 cm long and 25 cm diameter, large enough such that changes in chamber pressure and oxygen content were minimal during combustion of the thermoplastic sphere. The vacuum pump was used to evacuate the combustion products and facilitate the flushing and filling of the combustion chamber with the desired oxygen/nitrogen mixtures in the normal gravity tests. For the reduced gravity experiments, the overboard vent of the aircraft was used for operational convenience.

Experimental Conditions

Table 1 summarizes the experimental conditions. The sphere diameters were selected based on commercial availability and were limited to small diameters (less than 6.5 mm), to assure near-complete burning during the available duration of reduced gravity during the parabolic flights. Since pressure effects have been observed in the burning of liquid droplets (Mikami *et al.*, 1993; Vieille *et al.*, 1996), the effect of pressure was considered; however, safety constraints for the combustion chamber governed the upper pressure limit (0.15 MPa) for the experiments, whereas the lower pressure limit (0.05 MPa) was selected to ensure successful ignition of the spheres. Oxygen concentrations higher than 30 % were not considered in the test matrix because of the oxygen-clean requirements for the flight package;

oxygen level lower than 19 % were also not examined in the test matrix because the samples frequently failed to ignite (based on the observations from normal gravity experiments) using the current ignition technique.

Experimental Procedure

A test run involves the following steps: (1) the insertion of sample into the combustion chamber, (2) the flushing and venting of the chamber with the specified oxygen/nitrogen mixture three times, (3) the activation of the experiment during the low-G maneuver, and (4) the venting of combustion products and removal of sample holder. Most of the experimental steps were automated, except for manual operations of the video cameras, chamber venting and flushing, and sample insertion.

TABLE 1 Experimental test matrix

Material	Initial sphere diameter (D_o, mm)	Oxygen mole percent (X_O)	Total pressure (MPa)
PMMA	2.0, 2.5, 3.0, 3.2*, 4.8*, 6.4*	19.9, 21.0, 25.0, 30.0	0.05, 0.10, 0.15
PP	2.4, 3.0	21.0, 25.0, 30.0	0.05, 0.10
PS	3.0	25.0	0.05

* only used in the first flight experiments

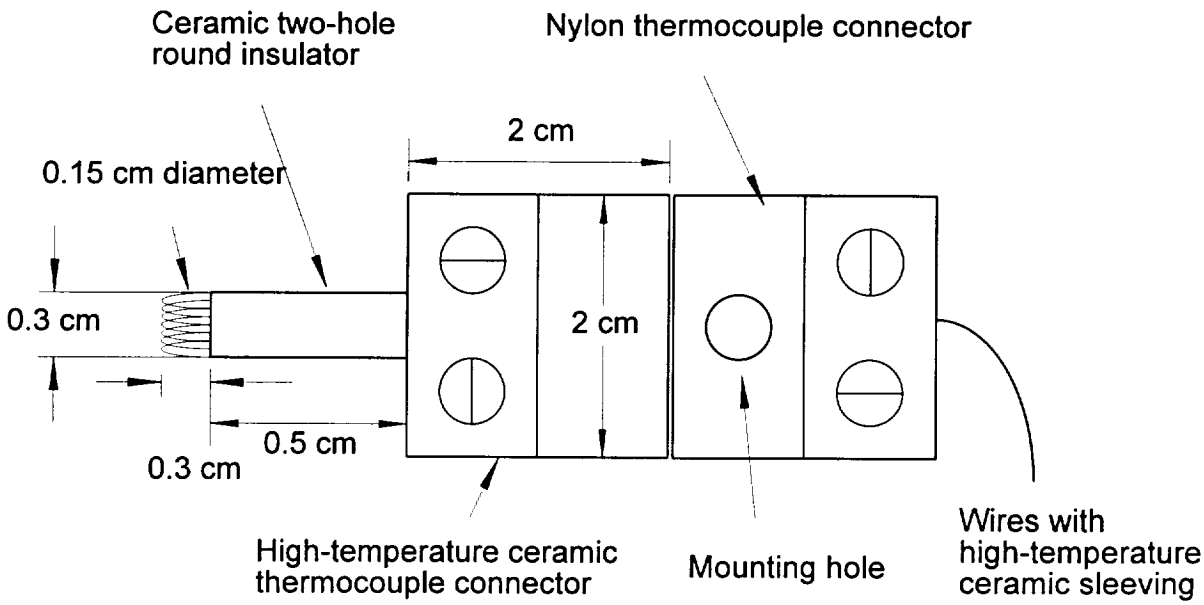

Figure 3. Schematic of the ignition coil.

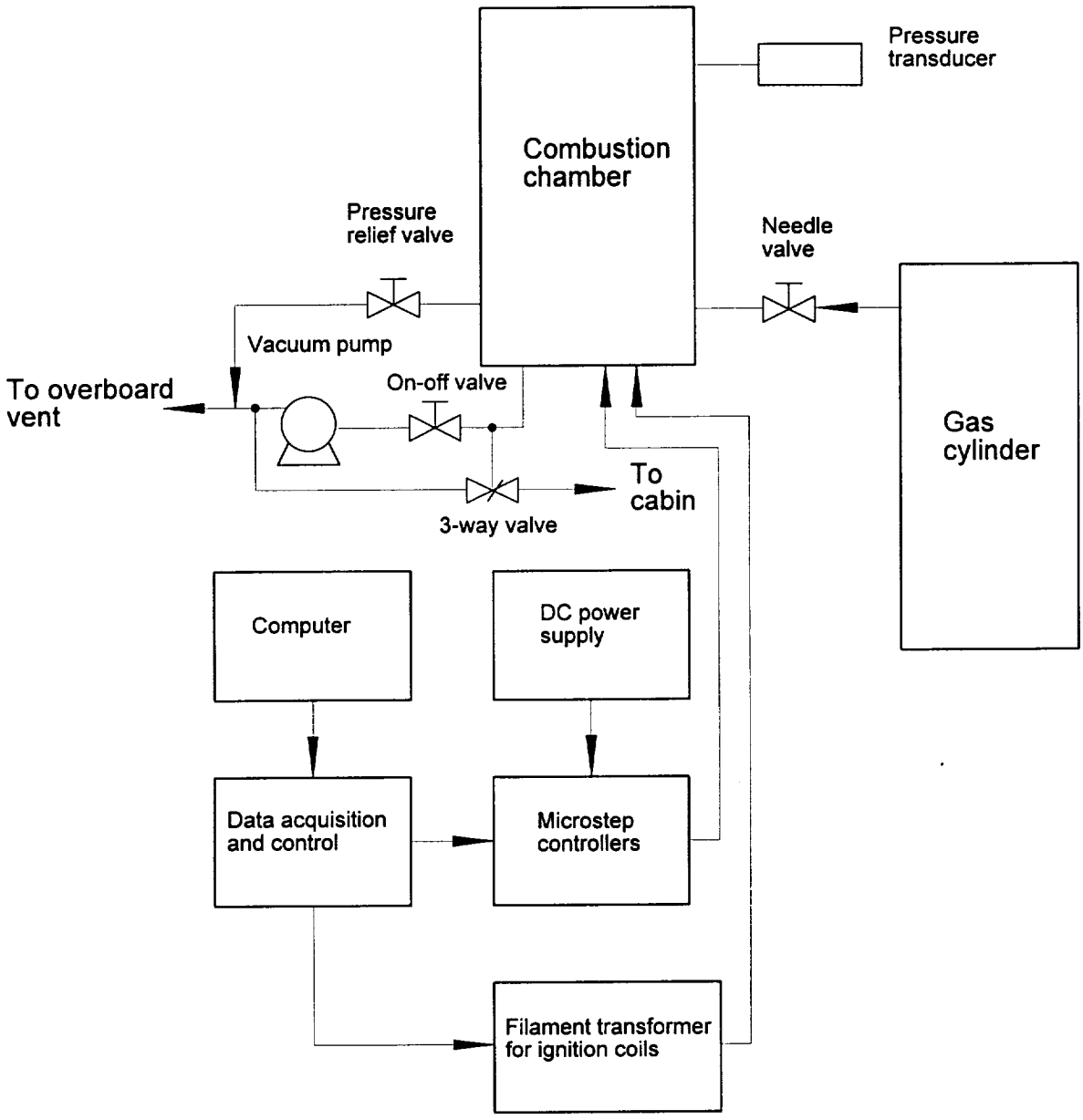

Figure 4. Flow diagram of the experimental set-up.

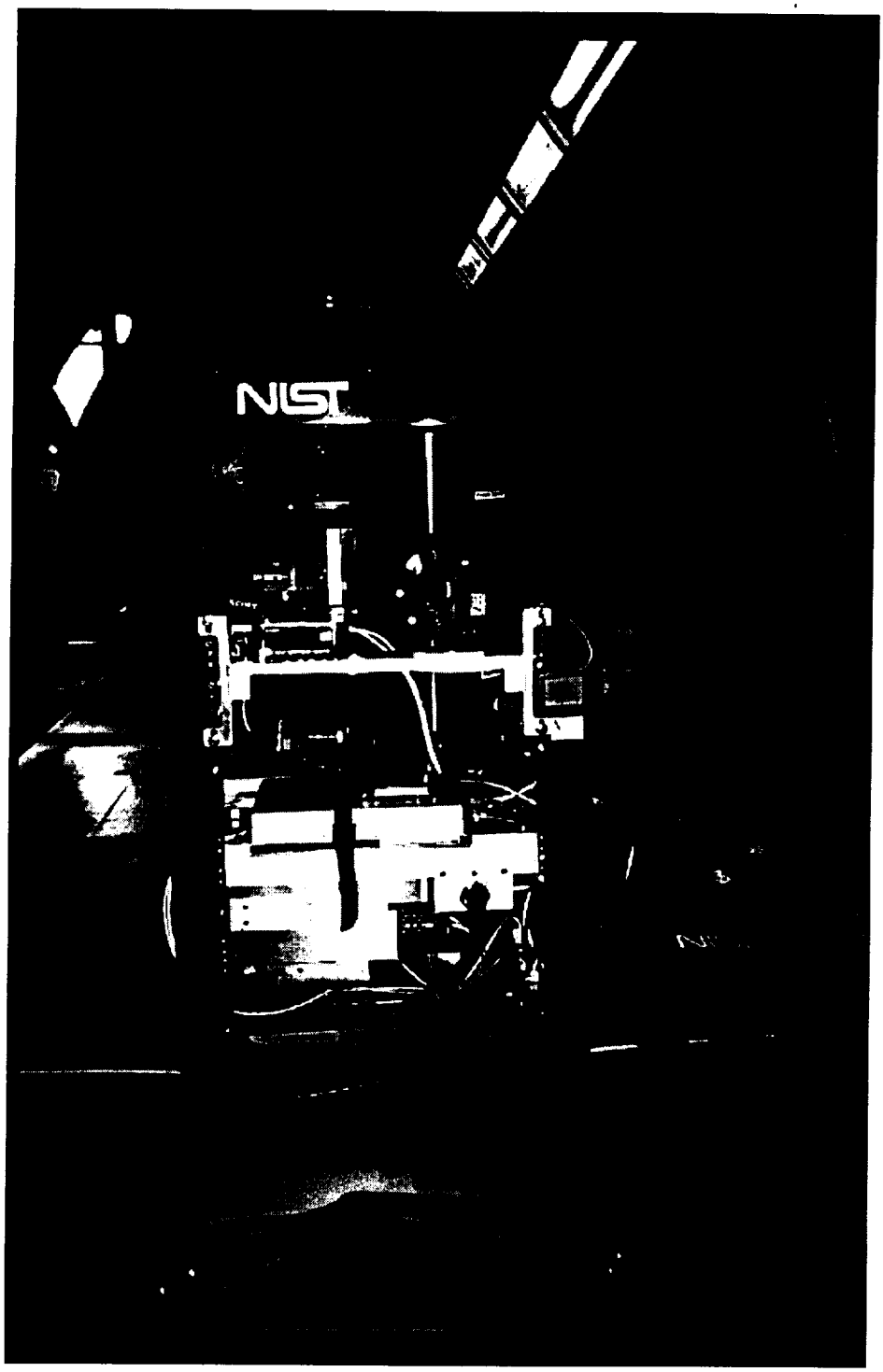

Figure 5. Experimental package.

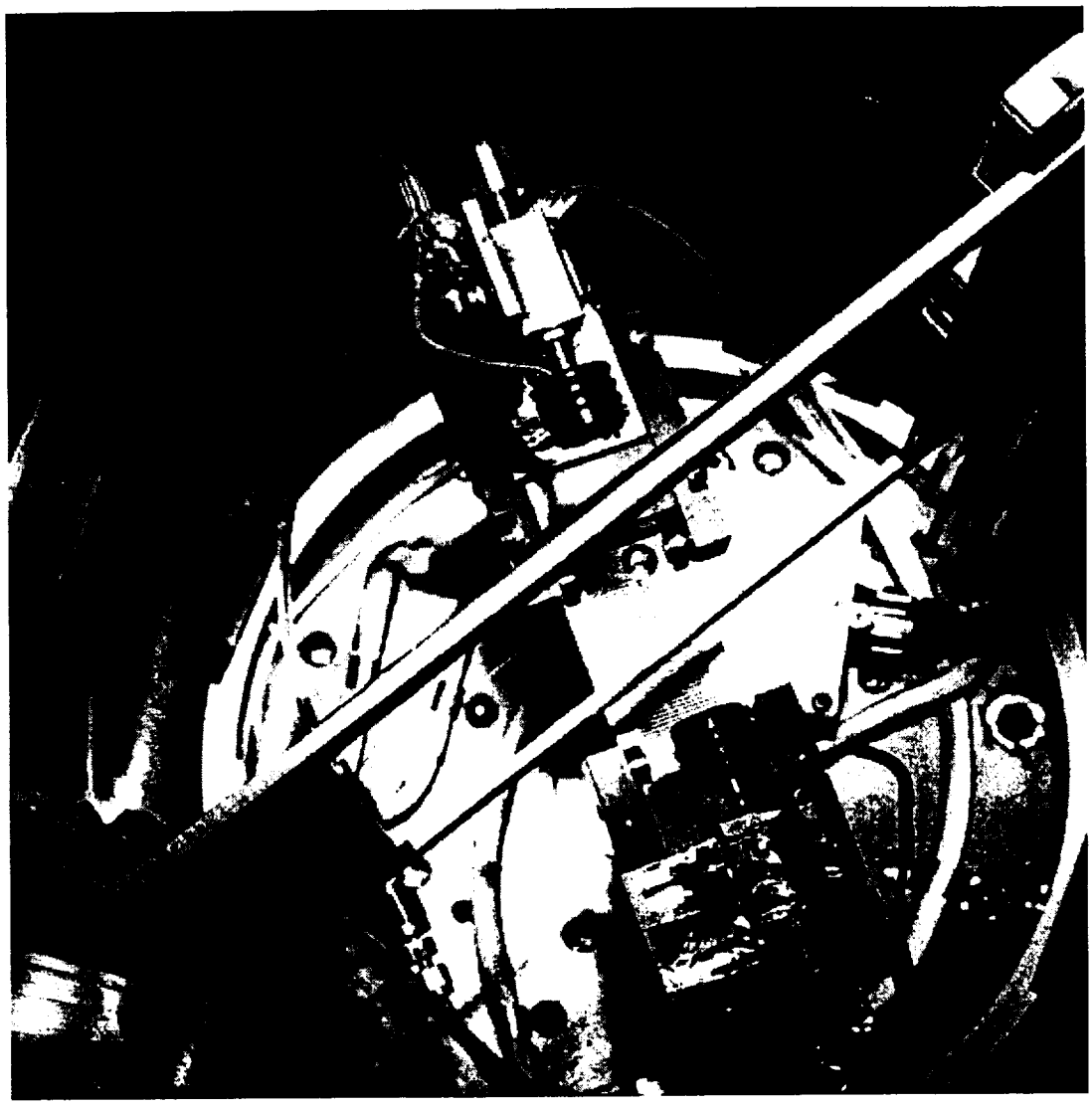

Figure 6. View of interior of combustion chamber showing a pair of micro-torches.

RESULTS AND DISCUSSION

Observations of the suspended sphere experiments in normal gravity can be summarized qualitatively as follows. Upon ignition, the sphere swelled and softened, and internal bubbling occurred. The violent ejection of material was not observed. The sphere shape deformed due to the action of gravity on the polymer melt, followed by dripping of the molten thermoplastic. Depending on the type of thermoplastic, the flames varied in luminosity and smoke. Finally, the deformed burning sphere fell off the suspension wire. This occurred in less than 10 s after ignition for all sphere diameters used in this study; and it was not possible to observe complete burning of the samples, making average burning rate measurements impractical. Figure 7 shows two images selected from the video recording of a PMMA sphere burning at normal gravity before and after the initiation of dripping of the polymer melt. The shape of the sample was significantly distorted from that of a sphere due to the influence of gravity as dripping occurred.

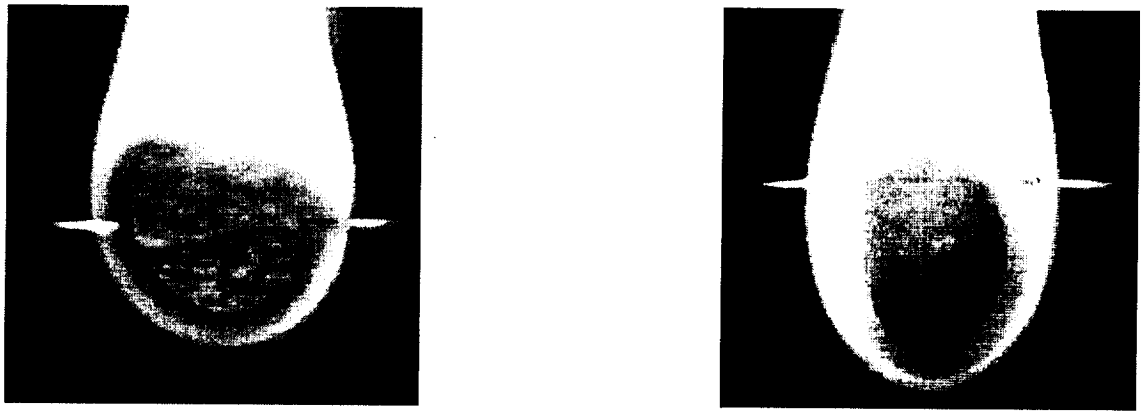

(a) (b)

Figure 7. Video images showing a PMMA sphere burning at normal gravity (D_o = 4.76 mm, 0.10 MPa, and 25 % O_2), before (a) and after (b) the occurrence of dripping of the polymer melt.

The period of reduced gravity provided by the NASA DC-9 and the KC-135 Reduced Gravity Aircraft was not long enough to obtain complete burning histories of spheres with initial diameters (D_o) greater than 3 mm for the range of conditions tested. For these large spheres (D_o > 3 mm), the diameter of the burning spheres did not appear to change significantly during the reduced gravity period. The mass loss due to burning was presumably balanced by increases in the apparent sphere diameter due to bubbling and swelling. For smaller spheres (D_o < 3 mm), complete combustion was observed. Flame extinction, a phenomenon frequently observed in liquid droplet microgravity combustion, was not observed in any of the sphere burning experiments.

Under reduced gravity conditions, experimental observations of the suspended PMMA spheres revealed a very different burning character. Figure 8 is a representative video sequence showing a 3 mm diameter PMMA sphere before and after ignition during reduced gravity. In Fig. 8, the components of the gravity vector (Gz, Gx, and Gy) are displayed at the bottom of each frame, while the date, time, and the parabolic trajectory number are displayed at the top of each frame. The sphere appeared to move randomly with respect to the suspension wire during combustion. The glowing ignition coil is seen in the first frame of the sequence. Ignition occurred approximately 3 s after the first frame and 2 s before the second. As the coil was retracted, it was de-energized and became less luminous. Upon ignition, the sample swelled and the outermost surface layer of the burning sample bubbled. A spherical blue flame was often observed, with its duration decreasing with total ambient pressure and oxygen concentration. The spherical flame subsequently became more luminous (yellowish in color), more bubbles nucleated, internal bubbling intensified, and a soot shell formed between the outer luminous flame and the thermoplastic sphere. Sputtering and ejection of material due to the bursting of bubbles from the burning sphere were observed, followed by break-up of the soot shell. The internal bubbling and ejection of material imparted momentum to the suspended sphere, causing it to exhibit impulsive motion and to slide along the support wire after melting had occurred through the sphere interior. The flame then lost its spherical shape, probably due to the motion of the sphere and G-jitter. The movement of the sample appeared to be more severe for spheres with a small initial diameter, possibly because of their smaller inertia and/or because of the rapid propagation of the molten front through the sphere. Although the ejection process temporarily perturbed the shape of the thermoplastic sphere in reduced gravity, the spherical shape tended to be restored. This was particularly true towards completion of fuel burning when the sphere diameter was small (small Grashof number), and motion of the suspended sphere was reduced (possibly due to surface tension effects).

Figure 9 is an enlarged video image of a burning PMMA sphere showing the break-up of a soot shell located between the luminous flame zone and the sphere surface. The formation of a soot shell is not surprising because the main PMMA degradation product is methylmethacrylate (Seshadri and William, 1978) which has a sooting character similar to that of heptane (exemplified by their nearly equal smoke heights, (Tewarson, 1988)), and soot shells have been observed during the combustion of heptane droplets at reduced gravity (Hara and Kumagai, 1990; Jackson *et al.*, 1992; Jackson and Avedisian, 1994). The break-up of the soot shell in the figure is reminiscent of the phenomena associated with a toluene droplet burning at reduced gravity with a small drift velocity (Avedisian *et al.*, 1988).

Although bubbling was observed during combustion in normal gravity, the ejection of molten material was not observed. Gravity-induced dripping of the melt appears to counteract the material ejection process because the transport of bubbles to the sphere surface is being resisted by the downward flow of the polymer melt. In terms of microgravity fire safety, the ejected burning material poses a potential ignition hazard to nearby flammable objects.

Figures 10 and 11 are representative video sequences showing burning 3 mm diameter polypropylene (PP) and polystyrene (PS) spheres, respectively, before and after ignition during parabolic flights. The combustion of PP and PS generally resembled that of PMMA; however, some salient differences were observed. A blue flame, observed immediately after ignition of PMMA, was not observed in the PP or PS flames. For PP, small burning particles were ejected through the flame from the parent sphere during combustion (see discussion below). There was less vibrating and sliding motion of the PP spheres along the wire than for the PMMA. The burning PS suspended sphere moved frequently with respect to the support wire. The flames were highly luminous. The spheres are not visible in Fig. 11 because of the intense flame luminosity, which suggests the presence of large quantities of soot particles, similar to that observed in normal gravity burning of PS

The video record suggests that the dynamic ejection events bear some resemblance to the phenomena of bursting of single bubbles at a gas/liquid interface, which has been described by Tomaides and Whitby (1976). It appears that there are two different dynamic ejection events playing a role in the burning of a thermoplastic in microgravity. The first type, which was observed during the combustion of the three thermoplastics, is a luminous flame protrusion attached to the parent flame surrounding the sphere. This type may be due to the release of gas jets associated with bubble bursting (Tomaides and Whitby, 1976). The second type, which was observed during PP combustion only, is the infrequent ejection of a burning material that is transported through the flame and beyond for some distance. This type may be due to the ejection of material from the breakup of a bubble jet (Tomaides and Whitby, 1976). The release of gas jets and the ejection of jet particles are clearly shown in Figure 10. Since the viscosity of the molten polymer depends on its molecular weight (Kashiwagi, 1994), the breakup of a bubble jet may be facilitated (in the case of PP) by a less viscous molten layer, a result of random scission of the polymer chain during thermal degradation (Cullis and Hirschler, 1981)

The velocities of the ejected material were estimated by tracking the material in two consecutive video frames. An ambiguity arises as to the direction of the ejected material relative to the two-dimensional view provided by the camera. Although two cameras were used, positioned 90° apart, the large number of ejection events and the time resolution precluded identifying individual tracks. Thus, a range of possible velocities was associated with each observation. If, however, the ejection process is assumed to be random with direction, then statistically, the actual velocity (V_a) is related to the measured velocity (V_m) as:

$$V_a = V_m \int_0^{\frac{\pi}{2}} \sec(\theta)\, d\theta = 1.56\, V_m$$

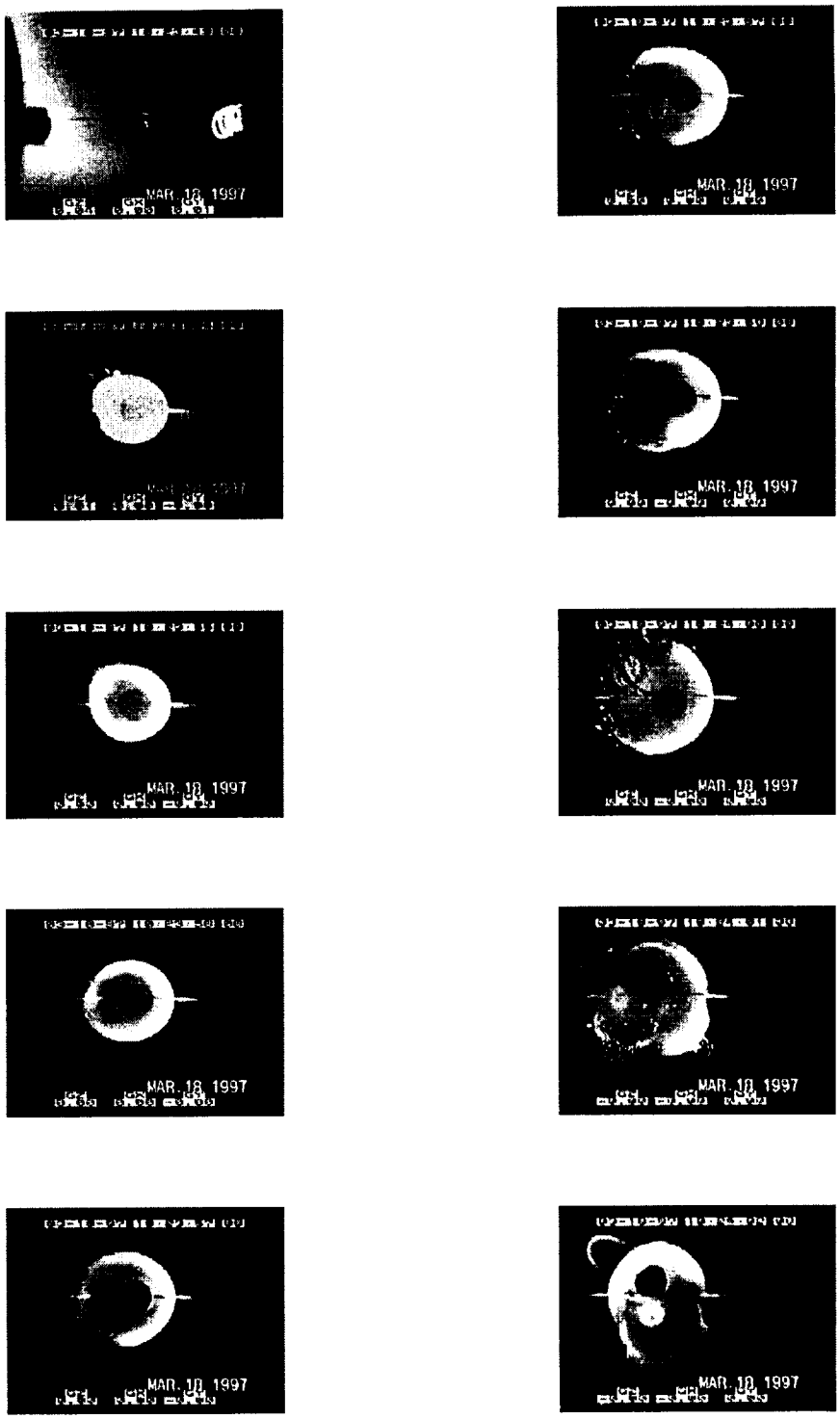

Figure 8. A video sequence (from top to bottom, and left to right) showing a PMMA sphere before and after ignition under reduced gravity conditions (D_o = 3 mm, 0.15 MPa, and 30% O_2); also shown is the energized-wire ignition device.

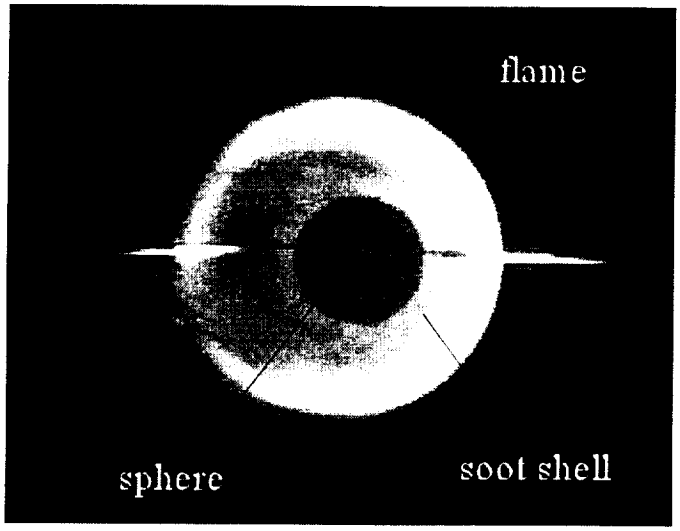

Figure 9. Break-up of a soot shell from a burning PMMA sphere under reduced gravity conditions (D_o = 3 mm, 0.15 MPa, and 30 % O_2).

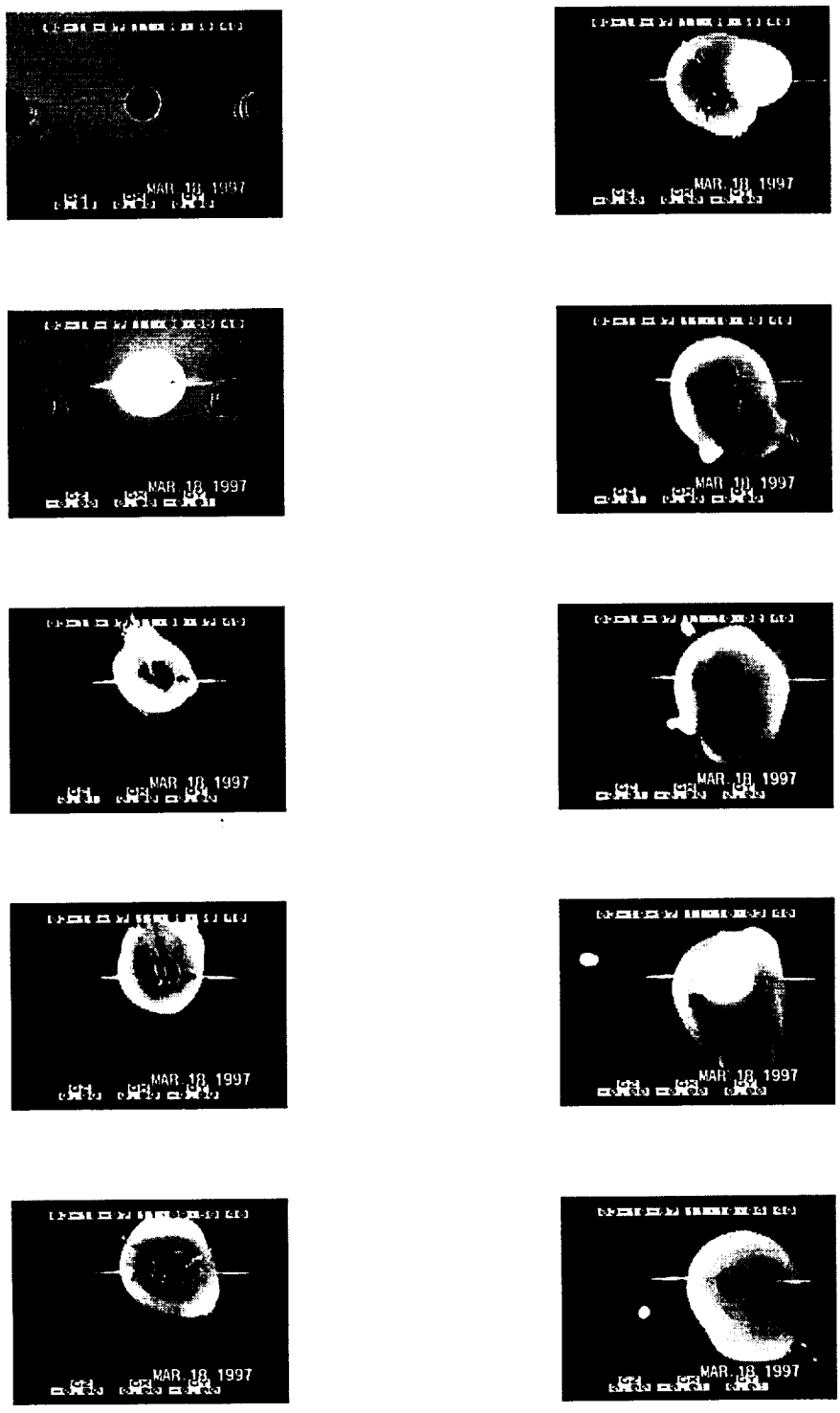

Figure 10. A video sequence (from top to bottom and left to right) showing a PP sphere before and after ignition under reduced gravity conditions (D_o = 3 mm, 0.10 MPa, and 30 % O_2).

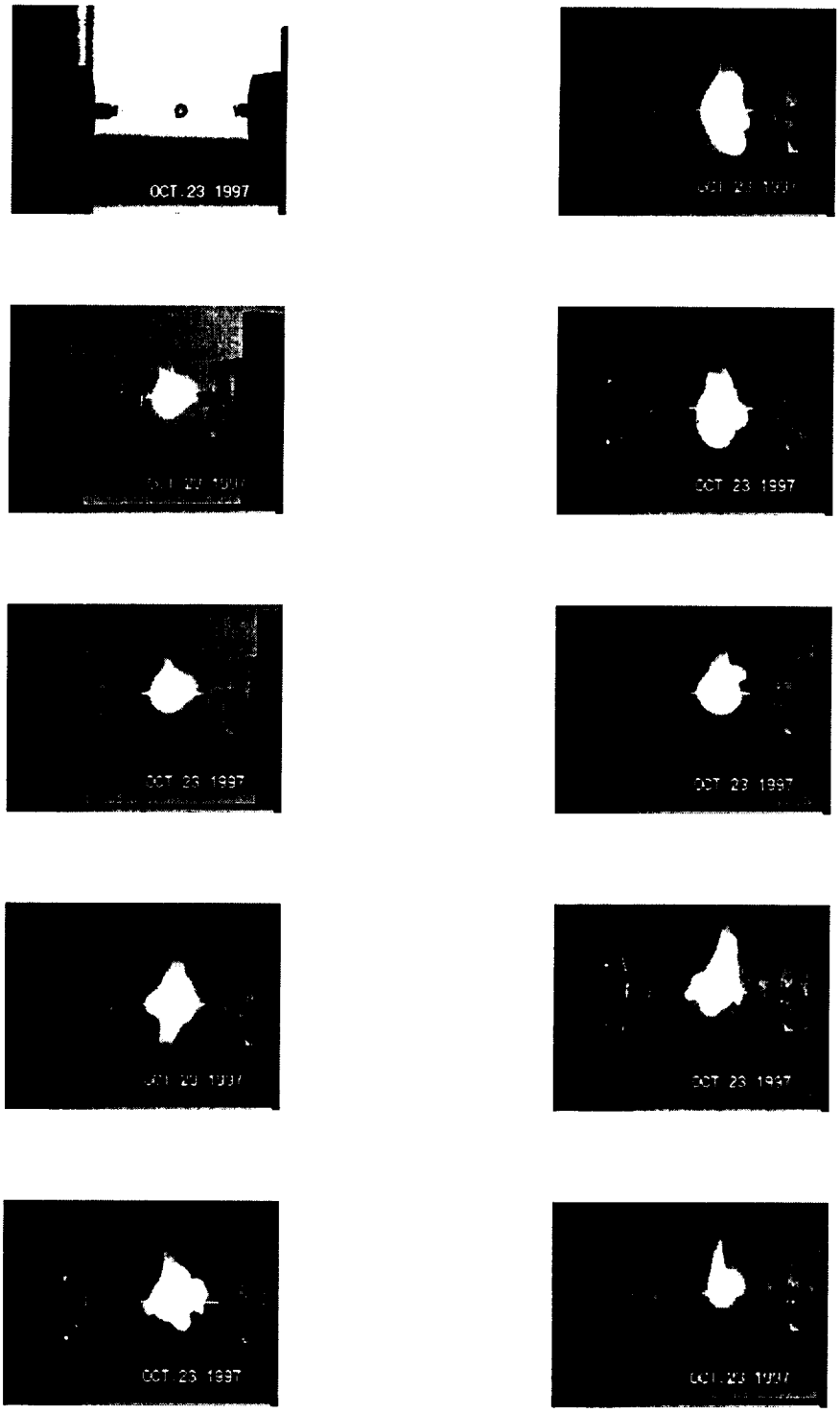

Figure 11. A video sequence (from top to bottom and left to right) showing a PS sphere before and after ignition under reduced gravity conditions (D_o = 3 mm, 0.05 MPa, and 25 % O_2).

For the PP spheres, V_a = 2.3 (± 1.2) cm/s (with 60 events observed). The ejected material appeared to decelerate at an average rate of ≈ 40 cm/s^2, and traverse an average distance of only ≈ 8 mm before burning to completion. V_a for PMMA and PS was not determined because the ejected material was never observed to exist beyond the visible flame of the parent sphere (see Figs. 8 and 11). However, the presence of ejection events was evident from instantaneous bulges in the visible flame of the (PMMA and PS) parent spheres (and the frequency of material ejection was determined). The average ejection frequency (E_f) is defined here as the number of ejection events divided by the total burning time of the sphere. The ejection frequency measurements did not differentiate between the two types of ejection events. Unlike the velocity, measurement of this parameter does not suffer from ambiguity associated with the two-dimensional view provided by the camera. Once ejection began, the ejection frequency tended to increase over the burning duration. The value of E_f was found to be sensitive to polymer type and independent of pressure. In addition, E_f tended to increase with oxygen concentration although the results are not statistically significant when experimental uncertainty is considered. It should be noted that the change in burn duration as the oxygen concentration varied was small (for example, see Fig. 6 where its value changes ≈ 15 %). The experimental uncertainty (dominated by variance) in the ejection frequency was much larger than this (≈ 30 %). The average value and the standard deviation of E_f were 3 Hz ± 1.5 Hz, 5 Hz ± 0.8 Hz, and 5 Hz ± 4 Hz for PMMA, PS, and PP, respectively.

Since the ejection of material and the ejection frequency are likely related to the formation and transport of bubbles in the polymer melt and bubble bursting at the sample surface, the pyrolysis rate may play a role in the ejection events. However, the mechanisms of bubble nucleation, growth, and transport in time-varying temperature and viscosity gradients are so complex, that it is difficult to interpret the ejection events simply based on global condensed-phase kinetics (Kashiwagi, 1994).

The diameter of the burning ejected material was obscured by the luminosity of its flame. In addition, an estimate of the diameter of the ejected material based on flame size has a very large uncertainty. It was possible, however, to determine an upper limit estimate of the mass of ejected material based on the observed burning duration of the ejected material (see below). It should be noted that bubble formation occurred at a much greater rate than E_f and that the release of vapor from bubble bursting is not easily estimated.

Figure 12 shows the temperature measurements obtained from suspending a 75 μm thermocouple wire with the junction initially located at the center of the sphere for conditions of 25 % oxygen and 0.10 MPa. The plateau in the temperature trace for D_o = 3.18 mm is the result of the thermocouple junction being displaced to the exterior of the sphere by impulsive motion. The sharp rise in the temperature is due to the sphere being dislodged from the suspending thermocouple during the ≈ 1.8 G maneuver of the aircraft. The non-existence of the plateau in the temperature trace for larger spheres, together with the video records, reaffirms the observation of less impulsive motion for larger spheres because the location of

the thermocouple junction remains relatively stationary with respect to the burning sphere and the melting front may not have propagated to the junction (*i.e.*, the junction is still embedded in solid phase polymer). Since the thermocouple junction was not fixed at the center of the sphere at all times during reduced gravity combustion, the interpretation of temperature measurement data was not meaningful, the thermocouple was not used in the rest of the flight experiments reported herein.

Burning Rate

Although the condensed-phase processes are complex, previous studies have successfully used the simple D^2-law to analyze results obtained from combustion experiments using polymer spheres in normal and reduced gravity (Essenhigh and Dreier, 1969; Waibel and Essenhigh, 1973; Raghunandan and Mukunda, 1977). The application of the D^2-law, which is an approach used to simplify the treatment of the condensed-phase processes, is based on the observation of an approximately linear relationship between the square of the sphere diameter and time in the experiments. The D^2-law can be written as:

$$D(t)^2 = D_o^2 - Kt \qquad (1)$$

where D is the time dependent sphere diameter, D_o is the initial diameter, K is the burning rate constant and t is the time. This law provides a heuristic explanation for the measurements made in this study. Figure 13 shows representative D^2 vs. time plots for 3 mm diameter PMMA spheres burning under various initial oxygen concentrations with an initial pressure of 0.10 MPa. These data were extracted from selected high contrast video images of the time-dependent diameter of the burning spheres. Figure 13 shows that for solid polymer spheres, the apparent burning behavior was characterized by two distinct periods: an initial period when the diameter increased slightly (approximately 10%), and a second final period when the diameter decreased fairly rapidly in a near-linear D^2 manner until complete burning was accomplished. For the data shown in Figure 13, Table 2 lists the observed duration of the first phase (t_1), and the sum of the initial and final periods, which is the time required for complete burning (t_b).

TABLE 2 Observed burning character of 3 mm PMMA spheres at $P = 0.10$ MPa for data corresponding to that shown in Figure 13

Initial oxygen mole percent (X_O)	Duration of initial phase (t_1, s)	Burn duration (t_b, s)	Average burning rate during Phase 2 (K_2, mm^2/s)
19.9	10.8	19.3	1.3
25	11.7	16.9	2.1
30	10.8	16.5	1.8

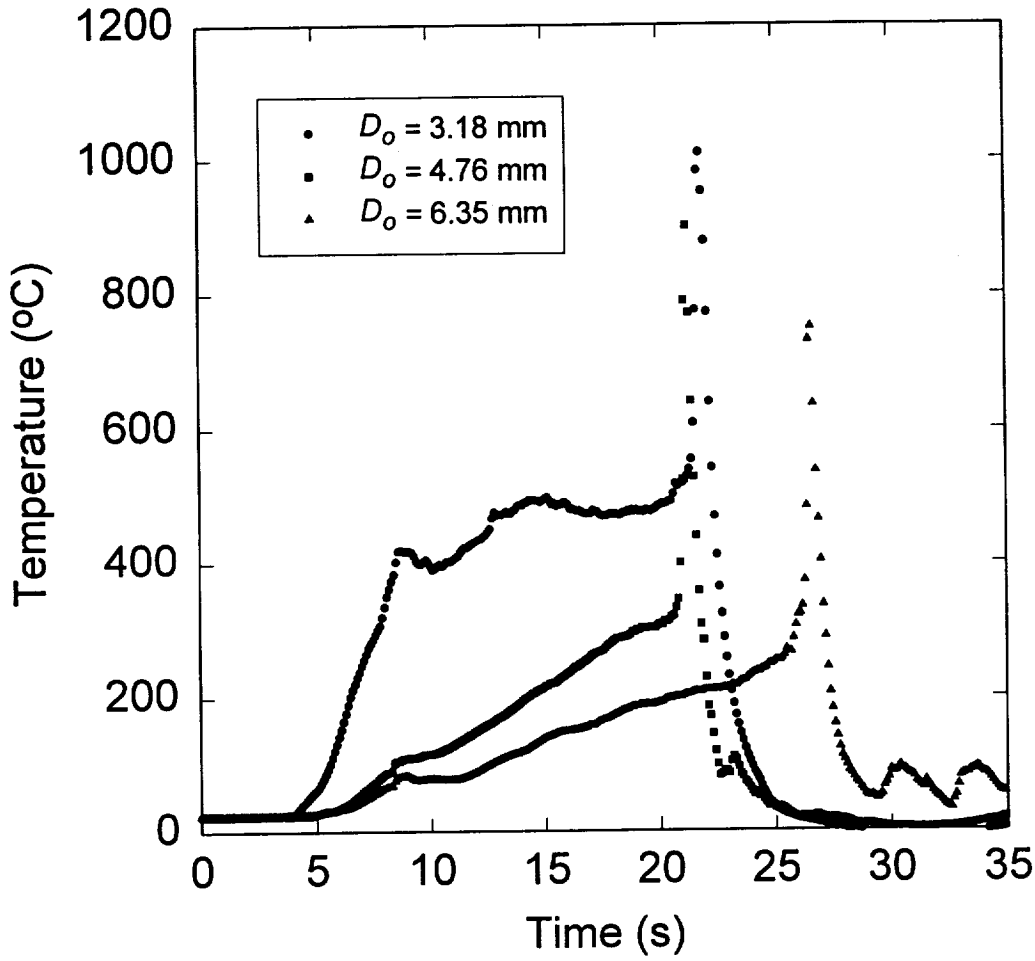

Figure 12. Temperature trace with thermocouple junction initially located at the center of a burning sphere with different D_o.

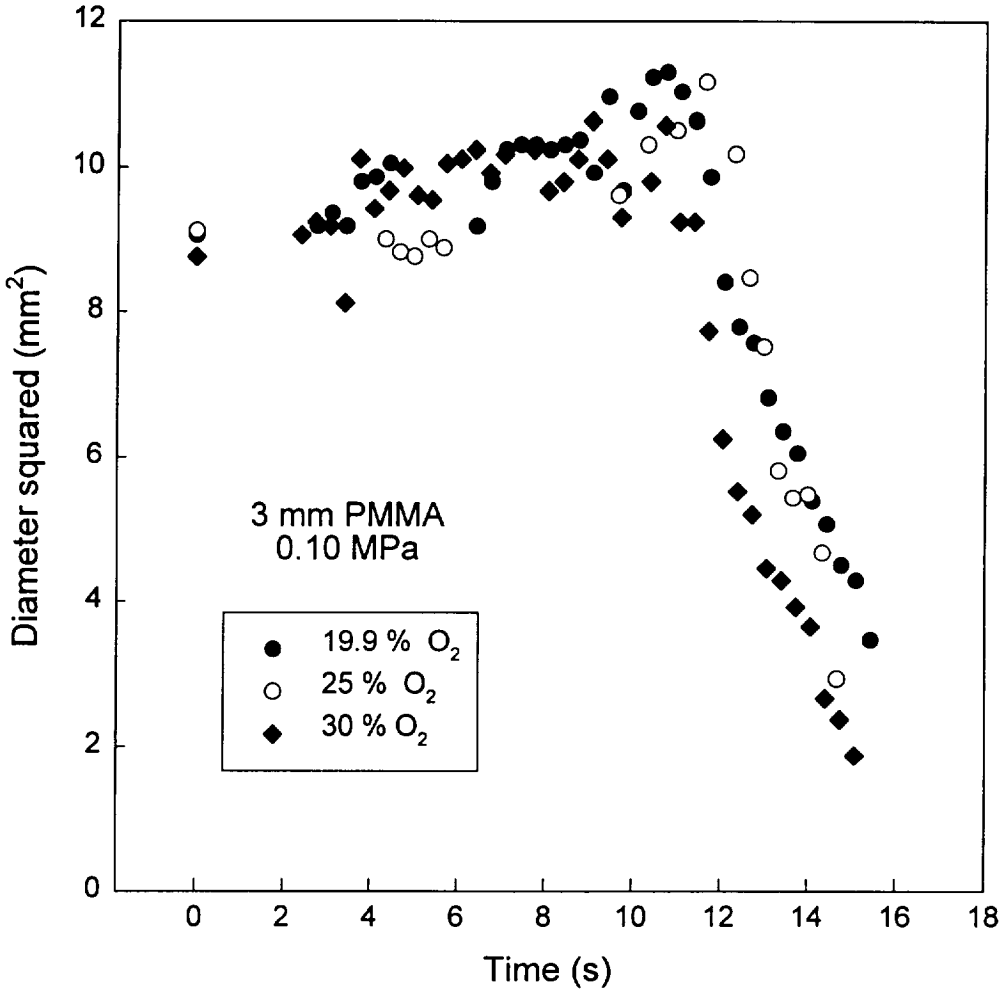

Figure 13. D^2 vs. time plots for 3 mm PMMA spheres with oxygen mole fractions of 19.9 %, 25 %, and 30 %, all with initial pressures of 0.10 MPa.

The apparent diameter of the sphere is due to a competition between diameter reduction due to mass loss from burning and sputtering, and diameter expansion due to the processes of swelling (density decrease with heating) and bubble growth. During the initial period, Figure 13 shows that the diameter increased only slightly, implying that mass loss was balanced by the expansion processes of swelling and bubbling. In ambient pressure liquid droplet burning, a similar phenomena associated with initial heating has been identified, when the droplet size hardly changes during a very short initial period (Law, 1982). A short heat-up period has also been observed in normal gravity combustion of small (< 2 mm) polymer spheres (Waibel and Essenhigh, 1973). In contrast to the liquid fuel heat-up period, the initial period of diameter expansion is generally very long for the solid fuels and conditions studied here, typically persisting for nearly half of the entire burn duration. For liquid droplet combustion, the slope of a best-fit line through a plot of D^2 versus time yields a burning rate constant. Because of the ambiguities associated with polymer bubbling and swelling, a time-averaged burning rate, determined over the entire combustion period, was used to characterize the polymer mass burning rate.

The time-averaged mass burning rate can be written as:

$$\dot{m}_{ave} = \frac{m_o}{t_b} = K m_o D_o^{-2} \qquad (2)$$

where m_o is the initial polymer mass, D_o is the initial diameter, and t_b is the burning duration. K is the average burning rate constant and is related to D_o and t_b:

$$K = \frac{D_o^2}{t_b} \qquad (3)$$

For a sphere, by definition: $m_o = \rho_o \pi \frac{D_o^3}{6}$ where ρ_o is the initial polymer density. For a given initial pressure and oxygen mole fraction (X_O), the time-averaged burning rate becomes:

$$\dot{m}_{ave} = (\frac{\pi}{6}) \rho_o D_o K \qquad (4)$$

Because of their impulsive motion and non-spherical flame shape, it was very difficult to obtain accurate measurements of the transient sphere and flame diameters from the video images. However, for a sphere that burns to completion over the reduced gravity period, the average burning rate constant K can be obtained from Eq. 3, using the measured burning duration (t_b). Similarly, the average mass burning rate ($\dot{m}_{ave}$) can be calculated using Eq. 2. The burn duration (t_b) was obtained from the video record using frame-by-frame analysis. Uncertainty in the measurement was less than 30 ms, leading to an uncertainty in the burning rate calculations of less than 2 %. The expanded uncertainty (σ)

for K was generally less than 10 %, with this value dominated by measurement variance. The results are summarized in Table 3, where the average mass burning rate and its uncertainty for PMMA are shown as a function of initial sphere diameter, oxygen concentration, and pressure. The number of runs in the table does not reflect the number of attempts in performing reduced-gravity experiments, but rather indicates the number of successful runs. Some data scatter is evident in the Table. For example, the 3 mm, 0.05 MPa results show a decreasing burning rate with oxygen concentration. The data scatter was likely due to a number of factors including (1) the low number of runs reported for some conditions; (2) the ejection of material from the polymer melt; and (3) difficulties in controlling the ignition process. For example, slight mis-positioning of the polymer spheres could cause preferential contact of the ignition coil with the polymer. Depending on the conditions, the 2 s ignition time was approximately 10 % to 20 % of the burning time. Unnecessarily prolonged contact of the heating coils with the sample surface may have increased the burning rate. Heat conduction along the suspended wire to the sphere interior may have also played a role, especially near the end of burning. The heat conduction along the support wire can be estimated by $\dot{Q}_{cond} \approx 2\, k_s \dfrac{T_f - T_s}{r_f - r} \pi R_1^2$, where k_s is the thermal conductivity of the wire, T_f is the flame temperature, T_s is the surface temperature of the sphere, r_f is the flame radius, r is the sphere radius, and R_1 is the radius of the wire. The factor 2 takes into account heat conduction into the sphere from the two directions. With k_s and R_1 fixed and assuming the flame front stand-off ratio $\dfrac{r_f}{r}$ ~ constant and $T_f - T_s$ ~ constant, then $\dot{Q}_{cond} \sim \dfrac{1}{r}$. Therefore, as $r \to 0$, $\dot{Q}_{cond}$ is comparable to $\dot{m} L$, where L is the latent heat of gasification. For finite r, however, an order of magnitude estimate shows that $\dot{Q}_{cond} << \dot{m} L$.

Despite the data scatter, several trends are apparent in Table 3: (1) the average burning rate increased with the initial sphere diameter; (2) the average burning rate increased with oxygen concentration; and (3) the average burning rate did not seem to be affected significantly by pressure (for the range of pressures studied here). Each of these observations is consistent with Equations 2 and 4. For a given X_O and pressure (K is constant), $\dot{m}_{ave} \sim D_o$. For a given D_o and pressure, $\dot{m}_{ave}$ increases with X_O because K increases with X_O. For given D_o and X_O, $\dot{m}_{ave}$ is relatively independent of the pressure because K is not sensitive to the range of pressures used here. The average mass burning rate of the PS spheres was also found to be proportional to the initial sphere diameter in normal gravity combustion studies (Panagiotou *et al.*, 1994)

Figure 14 shows the values of the average K and its standard deviation (σ) as a function of the initial oxygen concentration. Average values of K were determined using Eq. 3 and the data in Table 3. Since the average K does not significantly vary with pressure and D_o, all of the data in Table 3 were used to plot Figure 14. Also shown in Figure 14 are K values estimated using the B number (Law, 1982). The B number was calculated using an average flame temperature (≈ 1400 K) for the thermophysical properties, as recommended by

Law (1982), which is the average of the adiabatic flame temperature (2200 K) and the polymer surface temperature, measured in normal gravity as ≈ 640 K (Vovelle *et al*, 1987). As X_O varies, the B number takes values such that: $1 < B < 2$. Figure 14 shows that the relative trends in the reduced gravity PMMA burning rate measurements compare favorably to the trends estimated using the B number, although the absolute values differed by as much as 50 %.

Only a limited number of experiments were performed using PP and PS. Table 4 compares the average burning rate of PP and PS with those of PMMA for the *same* experimental conditions. The dependence of burning rate on oxygen concentration is also evident for PP spheres. The average burning rate of PMMA is significantly higher than that of PP and is similar to that of PS.

An upper limit estimate of the mass of ejected material for PP can be determined using Eq. 3, and assuming that the ejected material is condensed phase and that its density, $\rho_e \approx 1$ g/cm^3 (Troitzsch, 1983). Using K from Table 4, the mass of ejected material (m_e) can be estimated as $\approx 4/3\pi\ \rho_e (D_e/2)^3$, where D_e ($= \sqrt{K\, t_{be}}$) is the diameter of the ejected material and t_{be} is the observed duration of the burning of the ejected material. The total contribution to the burning rate for the ejected material is the product of the frequency of ejection (E_f) and the average mass for each ejection, $E_f\ m_e \approx 10^{-5}$ g/s (± 50 %) for PP (at 25 % O_2), which represents a small (≈ 1%) contribution to the overall burning rate. The large uncertainty is associated with the video framing rate and the short burning duration of the ejected material ($t_{be} \approx 2$ frames or 0.07 s). The contribution to the overall burning rate for ejections in the PMMA and PS spheres is smaller, if the ejections are due solely to the release of gaseous material.

Estimate of the Void Fraction of the Polymer Sphere

As the polymer sphere heats up, the processes of bubble nucleation and growth are responsible for the existence of gas-phase polymer degradation products that form a significant fraction of the sphere volume. The gas-phase void fraction of the burning polymer sphere was estimated by considering the sphere as a homogeneous two-phase mixture. Competing with the bubble formation processes are losses due to bubble release and evaporation from the polymer surface. The mass burning rate, $\dot{m}$, can be written as:

$$\dot{m} = -\frac{d}{dt}\left[\frac{4}{3}\pi \rho_d \left(\frac{D}{2}\right)^3\right] \qquad (5)$$

If the sphere is composed of bubbles of average density ρ_v and a solid melt of average density ρ_m and the sphere contains a time varying void volume fraction, $\alpha(t)$, then the sphere density (ρ_d) is:

$$\rho_d = \alpha \rho_v + (1-\alpha)\rho_m \qquad (6)$$

In Eq. (6), it is implicitly assumed that the solid sphere has reached a molten state upon ignition. This assumption is reasonable because a simple moving-boundary heat conduction calculation indicates that the melting front has almost penetrated to the center of the sphere within 2 seconds.

Substituting Eq. 6 into Eq. 5:

$$-\frac{6\dot{m}}{\pi D^3} = -(\rho_m - \rho_v)\frac{d\alpha}{dt} + \frac{3}{D}\frac{dD}{dt}\rho_d \qquad (7)$$

where the apparent diameter is controlled by the time-averaged mass loss and the transient void fraction.

As mentioned previously, the experimental results (*e.g.*, Figure 13) indicate that two distinct phases exist during burning of the polymer spheres. During the initial phase, the diameter is relatively constant, and during the second phase the square of the diameter linearly decreases with time until the sphere burns to completion at time t_b:

$$\frac{dD}{dt} \approx 0 \; ; \; D \approx D_o \quad for \quad 0 \le t \le t_1 \qquad (8)$$

$$D^2 = D(t=t_1)^2 - K_2 (t - t_1) \quad for \quad t_1 \le t \le t_2 \qquad (9)$$

During phase 2, K_2 is the average burning rate constant. If $t_1 = 0$, then $K_2 = K$ (where K is the burning rate constant over t_b as defined in Eq. 1. The initial condition for the diameter during phase 2 is: $D(t = t_1) \approx D_o$.

Applying the phase 1 conditions (Eq. 8) to the governing equation (Eq. 7) and assuming that the mass burning rate is constant ($\dot{m} \approx$ constant) and the void fraction is initially zero ($\alpha = 0$ at $t = 0$), obtains:

$$\alpha = \frac{6\dot{m}_{ave}\, t}{\pi D_o^3 (\rho_m - \rho_v)} \qquad 0 \le t \le t_1 \qquad (10)$$

TABLE 3 Summary of average PMMA burning rates (x 10^4 g/s) under various initial conditions

	0.05 MPa			
D_o (mm)	19.9 % O_2	21.0 % O_2	25.0 % O_2	30.0 % O_2
2.0	5.4 ± 0.4[a] (N[b] = 3)	5.8 ± 0.2 (N = 3)	7.5 ± 0.5 (N = 5)	6.7 ± 0.1 (N = 3)
2.5	6.4 ± 0.6 (N = 3)	7.5 (N = 1)	7.8 ± 0.4 (N = 5)	7.9 ± 0.8 (N = 3)
3.0	11.5 (N = 1)	10.2 ±3.9 (N = 2)	8.99 ± 0.50 (N = 4)	9.66 ± 0.18 (N = 3)
	0.10 MPa			
2.0	5.4 ± 0.4 (N = 3)	5.9 ± 0.6 (N = 5)	6.4 ± 0.6 (N = 4)	7.2 ± 0.2 (N = 3)
2.5	7.1 ± 0.3 (N = 3)	7.4 ± 0.5 (N = 5)	7.3 ± 0.1 (N = 3)	8.8 ± 0.4 (N = 3)
3.0	8.2 (N = 1)	8.6 ± 0.7 (N = 3)	9.4 ± 0.9 (N = 3)	10.2 ± 0.6 (N = 3)
	0.15 MPa			
2.0	6.2 ± 0.4 (N = 2)	5.6 ± 0.1 (N = 2)	6.8 ± 0.8 (N = 2)	6.9 ± 0.6 (N = 3)
2.5	6.5 (N = 1)	7.3 ± 0.2 (N = 2)	7.6 ± 0.3 (N = 2)	8.4 ± 0.6 (N = 3)
3.0	7.7 (N = 1)	8.5 ± 0.01 (N = 2)	9.1 ± 0.6 (N = 2)	10.0 ± 0.5 (N = 3)

[a] Mean ± standard deviation
[b] Number of runs

The assumption of constant $\dot{m}$ is reasonable because in combustion experiments at normal gravity using PMMA and PS spheres, mass loss was observed to decrease linearly with time for a significant portion of the total burning time (Waibel and Essenhigh, 1973; Raghunandan and Mukunda, 1977).

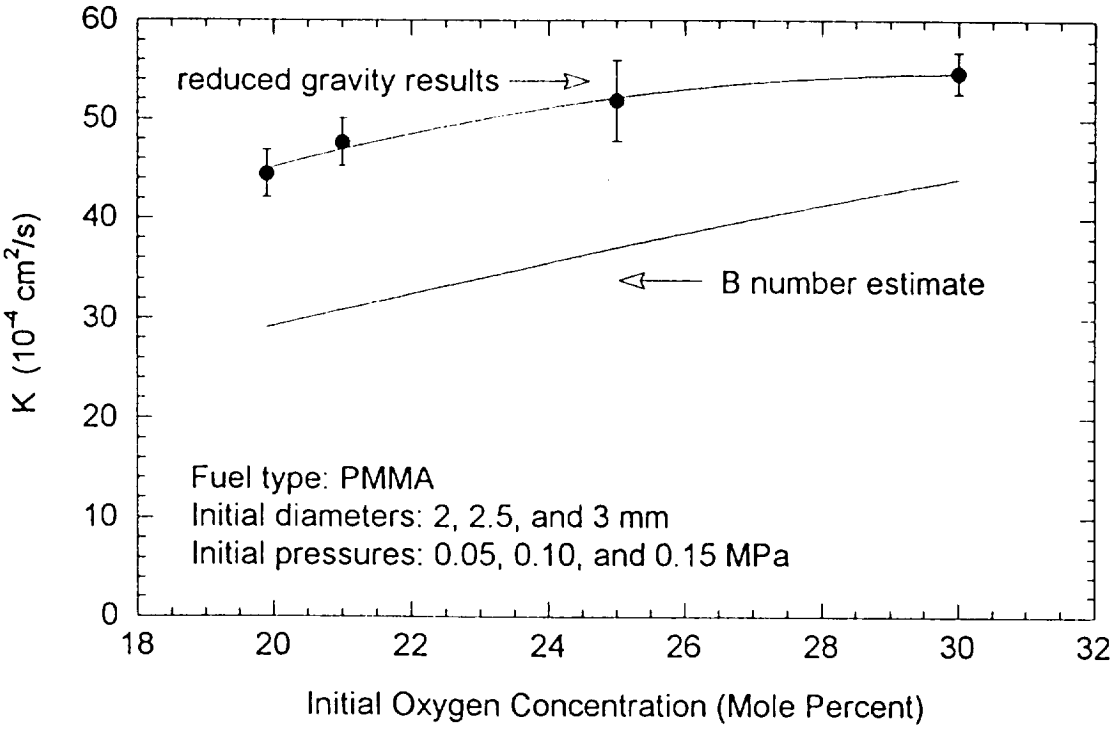

Figure 14. The average K and its standard deviation (σ) as a function of the initial oxygen concentration. Also shown are estimated K values using the B number.

TABLE 4 Comparison of average burning rates for different thermoplastics and initial conditions

Material	D_o (mm)	Oxygen (%)	Pressure (MPa)	N^a	$(\dot{m}_{ave} \pm \sigma)^b \cdot 10^4$ (g/s)
PMMA	3.0	30	0.10	3	10.2 ± 0.6
PP	3.0	30	0.10	2	7.0 ± 0.5
PMMA	3.0	25	0.10	3	9.4 ± 0.9
PP	3.0	25	0.10	1	5.81
PMMA	3.0	25	0.05	5	9.0 ± 0.5
PS	3.0	25	0.05	4	8.7 ± 0.8

[a] Number of runs
[b] Mean ± standard deviation

At the end of phase 1, Eq. 10 shows that:

$$\alpha(t=t_1) \equiv \alpha_1 = \frac{6\dot{m}_{ave}\, t_1}{\pi D_o^3 (\rho_m - \rho_v)} \qquad (11)$$

To evaluate α during phase 2, the derivative of the D^2 - law is determined:

$$\frac{dD}{dt} = \frac{1}{2}\frac{-K_2}{\sqrt{D_o^2 - K_2 (t-t_1)}} \qquad (12)$$

Introducing Eqs. 6 and 12 into Eq. 7, yields a first order differential equation in terms of α:

$$\frac{d\alpha}{dt} = \frac{3}{2}\frac{K_2 \alpha}{\left[D_o^2 - K_2 (t-t_1)\right]} + \frac{6\dot{m}_{ave}}{\pi(\rho_m - \rho_v)\left[D_o^2 - K_2 (t-t_1)\right]^{3/2}} - \frac{3K_2 \rho_m}{2\left[D_o^2 - K_2 (t-t_1)\right](\rho_m - \rho_v)} \qquad (13)$$

Integrating this relation and imposing the conditions (at $t = t_1$) defined by Eqs. 9 and 11 yields the solution for α during phase 2 (for $t_1 \leq t \leq t_b$):

$$\alpha = \frac{6\dot{m}_{ave}\, t}{\pi(\rho_m - \rho_v)\left[D_o^2 - K_2\,(t - t_1)\right]^{3/2}} + \frac{\rho_m}{(\rho_m - \rho_v)}\left\{ - \frac{D_o^3}{\left[D_o^2 - K_2\,(t - t_1)\right]^{3/2}}\right\} \qquad (14)$$

where t_1 (and thereby α_1 through Eq. 11) are empirically determined. The average PMMA melt density (ρ_m) for temperatures between ambient and 400 K was taken from Wittmann and Kovacs (1969). A linear extrapolation of that data was used for temperatures greater than 400 K. A polynomial fit to that data yields:

$$\rho_m\,(\mathrm{g/cm^3}) = 1.2042 - 5.0434\cdot10^{-4}\cdot T - 1.0437\cdot10^{-7}\cdot T^2$$

where T is in Celsius. The vapor phase density is assumed to be much smaller than the melt density, (*i.e.*, $\rho_v << \rho_m$).

Figure 15 shows the calculated void fraction (α) as a function of time from Eqs. 10 and 14 for the experiments corresponding to those shown in Figure 13, for 3 mm PMMA spheres with X_O = 19.9 %, 25.0 %, and 30.0 %. For those experiments, Table 2 lists t_1, t_b, and K_2. The PMMA density (ρ_m) is taken as 1 g/cm^3 in the calculation, which represents an average polymer melt temperature of 670 K. A sensitivity analysis showed that α is not strongly affected by changes in the melt density.

Figure 15 shows that bubbles are a significant, if not dominant, fraction of the sphere volume over most of the burning duration. The calculation results suggest that the void fraction increases with time, with between 60 % to 80 % of the sphere volume attributable to bubbles at t_1. In phase 2, the void fraction first levels off, and then rapidly increases until α = 1. The time when α = 1 can be interpreted as the burn-out time (t_b), when the melt has been completely vaporized. Figure 15 shows that the model predicts that t_b is equal to 16.0 s, 14.1 s, and 13.7 s for the data corresponding to that shown in Figure 13 with X_O = 19.9 %, 25.0 %, and 30.0 %, respectively. The calculated values of t_b are 2.8 s to 3.3 s shorter than the measured values (see Table 2), indicating the limitations of this simple homogeneous two-phase model. Still, the calculated results lend semi-quantitative insight into bubble behavior during the burning of a solid thermoplastic. The large value of the void fraction suggests that the mass loss mechanism associated with the escape of bubbles from the surface of the sphere (which includes sputtering), is likely to play a significant role in the burning rate, perhaps even superseding mass loss due to evaporation at the polymer surface. Measurement of the transient void fraction would guide refinement of the model. Such measurements are very challenging and remain to be accomplished.

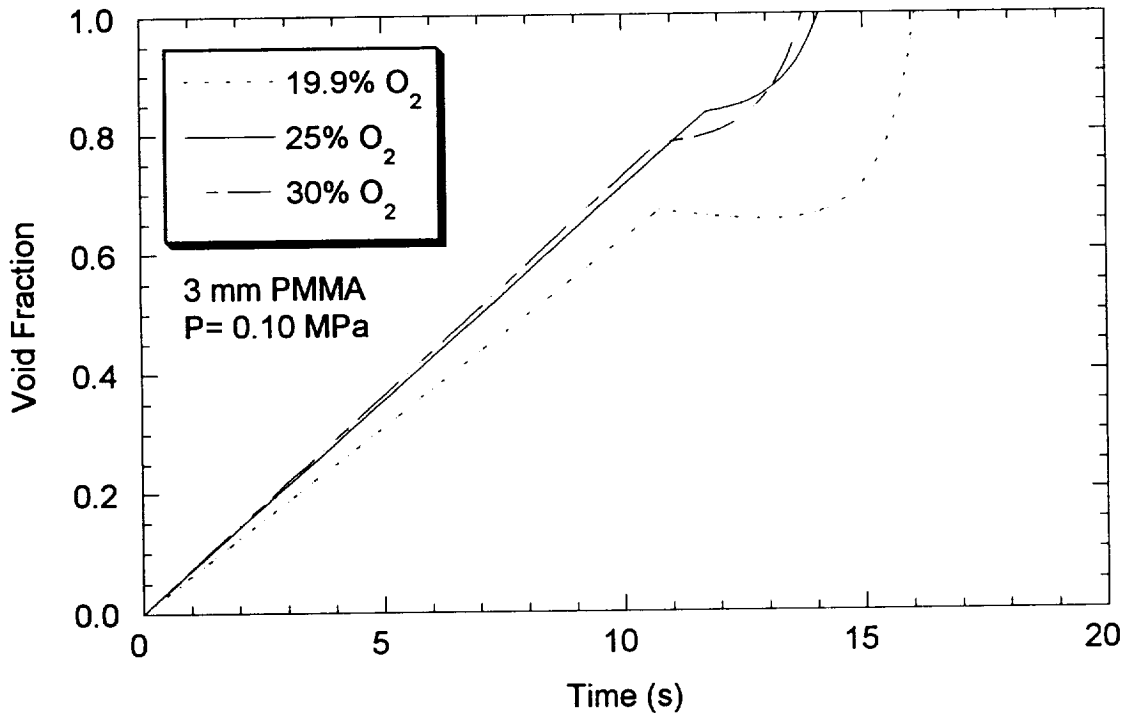

Figure 15. The calculated void volume fraction (α) corresponding to the data in Fig. 13.

CONCLUSIONS

The low gravity combustion experiments of thermoplastic (PMMA, PP, and PS) spheres reveal several interesting phenomena, which are not observed in normal gravity. Whereas dripping of a polymer melt can pose a fire hazard in normal gravity, in the case of PP, the random and violent ejection of burning material in microgravity represents a non-trivial fire safety challenge. If fire suppression strategies were based on normal gravity experimental results, serious consequences could result in a microgravity environment. The three thermoplastic types used in the reduced gravity experiments exhibited very different combustion characteristics. The two types of bubble bursting phenomena, the release of a gas jet and the ejection of condensed phase material from the break-up of a bubble jet, offer a plausible explanation for the dynamic ejection events during combustion of the three types of polymers studied here. The average burning rates of PMMA were found to increase with the initial sphere diameter and oxygen concentration and were not affected significantly by pressure. Under the same initial conditions, the average burning rate of PP was lower than PMMA, whereas the burning rate of PS was similar to PMMA.

Calculations show that during burning, a large fraction of the sphere is composed of gaseous bubbles that nucleate, grow and escape from the polymer, causing sputtering of molten burning solid polymer. Unlike liquid droplets, diameter expansion of the molten fuel occurs mainly due to the in-depth formation and growth of bubbles, whereas the decreased density accompanying polymer heating also contributes. Sputtering and the escape of bubbles from the sphere surface act to enhance the mass loss rate of polymer burning.

Based on the observations of the suspended burning spheres and some of the experiments in reduced gravity wherein unsupported burning spheres were *accidentally* created due to broken suspended wires, experiments using unsupported spheres may prove to be not feasible because the impulsive motion of the sphere imparted by the spluttering and ejection of molten material can cause the unsupported sphere to drift out of the field of view of the cameras, making observations impossible.

Further experiments obtained under better reduced gravity environment (freely-floating experiments aboard the aircraft) are needed to improve the repeatability of the experimental data so that the burning rate results can be used with better confidence in future model validation. The material properties and molecular weights of these polymers should be well characterized in future studies because the burning rates are affected by these properties.

REFERENCES

Avedisian C. T., Yang, J. C., and Wang, C. H., "On Low Gravity Droplet Combustion," *Proc. Roy. Soc. London*, **A 420**: 183-200 (1988).

Aseeva, R.M. and Zaikov, G.E., *Combustion of Polymer Materials*, Hanser Publisher, Munich, 1985.

Butler, K., "Numerical Modeling for Combustion of Thermoplastic Materials in Microgravity," *Fourth International Microgravity Combustion Workshop*, pp. 249-254, Cleveland, Ohio, May 19-21, 1997.

Chung, S.L. and Tsang, S.M., "Soot Control During the Combustion of Polystyrene," *J. Air Waste Manage. Assoc.*, **41**: 821-826 (1991).

Chung, S.L. and Lai, N.L., "Suppression of Soot by Metal Additives During the Combustion of Polystyrene," *J. Air Waste Manage. Assoc.*, **42**:1082-1088 (1992).

Cullis, C.F. and Hirschler, M.M., *The Combustion of Organic Polymer*, Clarendon Press, Oxford, 1981.

Essenhigh, R.H. and Dreier, W.L., "Combustion Behavior of Thermoplastic Polymer Spheres Burning in Quiescent Atmosphere of Air," *Fuel*, **48**:330-342 (1969).

Friedman, R., "Fire Safety in Spacecraft," *Fire & Materials*, **20**:235-243 (1996).

Goldmeer, J.S., Urban, D.L., and T'ien, J.S., "An Experimental Study of Solid Diffusion Flame Extinction and Transition to Microgravity," *Eastern States Section of the Combustion Institute, Fall Technical Meeting*, Princeton University, Princeton, NJ, October 25-27, 1993, pp. 441-444.

Goldmeer, J.S., T'ien, J.S., and Urban, D.L., *Fourth International Microgravity Combustion Workshop*, pp. 435-440, Cleveland, Ohio, May 19-21, 1997.

Hara, H., and Kumagai, S., "Experimental Investigation of Free Droplet Combustion Under Microgravity," *Twenty-third Symposium (International) on Combustion*, The Combustion Institute, Pittsburgh, 1990, pp. 1605-1610.

Hertzberg,.M., Conti, R.S., and Cashdollar, K.L., "Spark Ignition Energies for Dust-Air Mixtures: Temperature and Concentration Dependences," *Twentieth Symposium (International) on Combustion*, The Combustion Institute, Pittsburgh, 1984, pp. 1681-1990.

Jackson, G.S., Avedisian, C. T., and Yang, J.C., "Observations of Soot During Droplet Combustion at Low Gravity: Heptane and Heptane/Monochloro-alkanes Mixtures," *Int. J. Heat & Mass Transfer*, **35**: 2017-2033 (1992).

Jackson, G.S. and Avedisian, C.T., "The Effect of Initial Diameter in Spherically Symmetric Droplet Combustion of Sooting Fuels," *Proc. Roy. Soc. London* **A 446**:255-276 (1994).

Kashiwagi, T., "Polymer Combustion and Flammability - Role of the Condensed Phase," *Twenty-Fifth Symposium (International) on Combustion*, The Combustion Institute, Pittsburgh, 1994, pp. 1423-1437.

Kobayashi, H., Ono, N., Okuyama, Y., and Niioka, T., "Flame propagation Experiment of PMMA Particle Cloud in a Microgravity Environment," *Twenty-Fifth Symposium (International) on Combustion*, The Combustion Institute, Pittsburgh, 1995, pp. 1693-1699.

Law, C.K., "Recent Advances in Droplet Vaporization and Combustion," *Prog. Energy Combust. Sci.* **8**: 171-201 (1982).

Melikhov, A.S., Potyakin, V.I., Ryzhov, A.M., and Ivanov, B.A., "Limiting Polymer Combustion Regimes in the Absence of Free Convection," *Comb. Expl. & Shock Waves*, **19**: 393-395 (1983).

Mikami, M., Kono, M., Sato, J., Dietrich, D.L., and Williams, F.A., "Combustion of Miscible Binary-Fuel Droplets at High Pressure under Gravity," *Combust. Sci. and Tech.*, 90:111-123 (1993).

Okajima, S., Kawakami, T., and Raghunandan, B. N., "Extinction of Fuel Particles Burning Under Microgravity," Work-in-Progress Poster Session, *Twenty-Sixth Symposium (International) on Combustion*, The Combustion Institute, Pittsburgh, 1996.

Okuyama, Y., Ohtomo, Y., Maruta, K., Kobayashi, H., and Niioka, T., "An Experimental Study on Particle-Cloud Flames in a Microgravity Field," *Twenty-Sixth Symposium (International) on Combustion*, The Combustion Institute, Pittsburgh, 1996, pp. 1369-1375.

Olson, S.L. and Hegde, U., "Imposed Radiation Effects on Flame Spread over Black PMMA in Low Gravity," *Eastern States Section of the Combustion Institute, Fall Technical Meeting*, Clearwater Beach, FL, December 5-7, 1994, pp.348-351.

Panagiotou, T. and Levendis, Y., "A Study of Combustion Characteristics of PVC, Poly(styrene), Poly(ethylene), and Poly(propylene) Particles under High Heating Rates," *Comb. Flame*, **99**: 53-74 (1994).

Panagiotou, T., Levendis, Y., and Delichatsios, "Combustion Behavior of Poly(Styrene) Particles of Various Degree of Crosslinking and Styrene Monomer Droplets," *Comb. Sci. Tech.*, **103**: 63-84 (1994).

Panagiotou, T. and Levendis, Y., "Observations on the Combustion of Pulverized PVC and Poly(ethylene)," *Comb. Sci. Tech.*, **112**: 117-140 (1996).

Raghunandan, B.N. and Mukunda, H.S., "Combustion of Polystyrene Spheres in Air," *Fuel*, **56**: 271-276 (1977).

Seshadri, K., and Williams, F.A., "Structure and Extinction of Counterflow Diffusion Flames above Condensed Fuels: Comparison between Poly(methyl Methacrylate) and Its Liquid Monomer, Both Burning in Nitrogen-Air Mixtures," *J. Polymer Science*, **16**: 1755-1778, (1978).

Tewarson, A., "Smoke Point Height and Fire Properties Materials," NIST-GCR-88-555 (1988).

Tomaides, M. and Whitby, K.T., "Generation of Aerosols by Bursting of Single Bubbles," in *Fine Particles, Aerosol Generation, Measurement, Sampling, and Analysis*, B.Y.H. Liu (ed.), Academic Press, New York, 1976.

Troitzsch, J., *International Plastics Flammability Handbook, Principles-Regulations-Testing and Approval*, Macmillan Publishing, New York, 1983.

Vieille, B., Chauveau, C., Chesneau, X., Odeïde, A., and Gökalp, I., "High Pressure Droplet Burning Experiments in Microgravity," *Twenty-Sixth Symposium (International) on Combustion*, The Combustion Institute, Pittsburgh, 1996, pp. 1259-1265.

Vovelle, C., Delfau, J.L., Reuillon, M., Bransier, Q., and Laraqui, N., "Experimental and Numerical Study of the Thermal Degradation of PMMA," *Combust Sci Tech.*, **53**: 187-201 (1987).

Waibel, R.T. and Essenhigh, R.H., "Combustion of Thermoplastic Polymer Particles in Various Oxygen Atmospheres: Comparison of Theory and Experiment," *Fourteenth Symposium (International) on Combustion*, The Combustion Institute, Pittsburgh, 1973, pp. 1413-1420.

Wendt, J.O., "Fundamental Coal Combustion Mechanisms and Pollutant Formation in Furnaces," *Prog. Energy Combust. Sci.*, **6**: 201-222 (1980).

Wichman, I.S., "A Model Describing the Steady-State Gasification of Bubble-Forming Thermoplastics in Response to an Incident Heat Flux," *Comb. Flame*, **63**: 217-229 (1986).

Williams, F.A., *Combustion Theory*, Benjamin-Cummings, Menlo Park, CA, 1985.

Wittmann, J.C., and Kovacs, A.J., "Influence de la Stereorégularite des Chaines sur les Transitions du Polyméthacrylate de Méthyle," *J. Polymer Sci.*, Part C, **16**: 4443-4452 (1969).

Yang, J. C., and Hamins, A., "Combustion of a Polymer (PMMA) Sphere in Microgravity," *Third International Microgravity Combustion Workshop*, pp. 115-120, Cleveland, Ohio, April 11-13, 1995.

Yang, J.C., Hamins, A., Glover, M., and King, M., "Experimental Observations of PMMA Spheres Burning at Reduced Gravity," *Fourth International Microgravity Combustion Workshop*, pp. 243-248, Cleveland, Ohio, May 19-21, 1997.

REPORT DOCUMENTATION PAGE

Form Approved
OMB No. 0704-0188

1. AGENCY USE ONLY (*Leave blank*)	2. REPORT DATE	3. REPORT TYPE AND DATES COVERED
	December 1999	Final Contractor Report

4. TITLE AND SUBTITLE

Combustion of a Polymer (PMMA) Sphere in Microgravity

5. FUNDING NUMBERS

WU-962-22-00-00
Interagency Agreement
C-32017-C

6. AUTHOR(S)

Jiann C. Yang, Anthony Hamins, and Michelle K. Donnelly

7. PERFORMING ORGANIZATION NAME(S) AND ADDRESS(ES)

National Institute of Standards and Technology
Building and Fire Research Laboratory
Gaithersburg, Maryland 20899

8. PERFORMING ORGANIZATION REPORT NUMBER

E-11925

9. SPONSORING/MONITORING AGENCY NAME(S) AND ADDRESS(ES)

National Aeronautics and Space Administration
John H. Glenn Research Center at Lewis Field
Cleveland, Ohio 44135-3191

10. SPONSORING/MONITORING AGENCY REPORT NUMBER

NASA CR—1999-209403
NISTIR 6331

11. SUPPLEMENTARY NOTES

Project Manager, H. Ross, Microgravity Science Division, NASA Glenn Research Center, organization code 6700, (216) 433-2562.

12a. DISTRIBUTION/AVAILABILITY STATEMENT

Unclassified - Unlimited
Subject Categories: 29 and 31 Distribution: Nonstandard

This publication is available from the NASA Center for AeroSpace Information, (301) 621-0390.

12b. DISTRIBUTION CODE

13. ABSTRACT ***(Maximum 200 words)***

A series of low gravity, aircraft-based, experiments was conducted to investigate the combustion of supported thermoplastic polymer spheres under varying ambient conditions. The three types of thermoplastic investigated were polymethylmethacrylate (PMMA), polypropylene (PP), and polystyrene (PS). Spheres with diameters ranging from 2 mm to 6.35 mm were tested. The total initial pressure varied from 0.05 MPa to 0.15 MPa whereas the ambient oxygen concentration varied from 19 % to 30 % (by volume). The ignition system consisted of a pair of retractable energized coils. Two CCD cameras recorded the burning histories of the spheres. The video sequences revealed a number of dynamic events including bubbling and sputtering, as well as soot shell formation and break-up during combustion of the spheres at reduced gravity. The ejection of combusting material from the burning spheres represents a fire hazard that must be considered at reduced gravity. The ejection process was found to be sensitive to polymer type. All average burning rates were measured to increase with initial sphere diameter and oxygen concentration, whereas the initial pressure had little effect. The three thermoplastic types exhibited different burning characteristics. For the same initial conditions, the burning rate of PP was slower than PMMA, whereas the burning rate of PS was comparable to PMMA. The transient diameter of the burning thermoplastic exhibited two distinct periods: an initial period (enduring approximately half of the total burn duration) when the diameter remained approximately constant, and a final period when the square of the diameter linearly decreased with time. A simple homogeneous two-phase model was developed to understand the changing diameter of the burning sphere. Its value is based on a competition between diameter reduction due to mass loss from burning and sputtering, and diameter expansion due to the processes of swelling (density decrease with heating) and bubble growth. The model relies on empirical parameters for input, such as the burning rate and the duration of the initial and final burning periods.

14. SUBJECT TERMS	15. NUMBER OF PAGES
Combustion; Fire safety; Polymers; Polymethlymethacrylate; Polypropylene; polystyrene	47
	16. PRICE CODE A03

17. SECURITY CLASSIFICATION OF REPORT	18. SECURITY CLASSIFICATION OF THIS PAGE	19. SECURITY CLASSIFICATION OF ABSTRACT	20. LIMITATION OF ABSTRACT
Unclassified	Unclassified	Unclassified	